JOURNAL OF VIROLOGY, May 1994, p. 3267–3282
0022-538X/94/$04.00+0

Vol. 68, No. 5

Identification of a Dimerization Domain in the C-Terminal Segment of the IE110 Transactivator Protein from Herpes Simplex Virus

DOLORES M. CIUFO,[1] MARY-ANN MULLEN,[2]† AND GARY S. HAYWARD[1,2]*

The Virology Laboratories, Department of Pharmacology and Molecular Sciences,[2] and Department of Oncology,[1] Johns Hopkins University School of Medicine, Baltimore, Maryland 21205

Received 8 October 1993/Accepted 2 February 1994

The 775-amino-acid IE110 (or ICP0) phosphoprotein of herpes simplex virus (HSV) functions as an accessory transcription factor during the lytic cycle and plays a critical role in reactivation from latent infection. By immunofluorescence analysis, IE110 localizes in a novel pattern consisting of several dozen spherical punctate granules in the nuclei of DNA-transfected cells. We constructed a hybrid version of IE110 that contained an epitope-tagged domain from the N terminus of the HSV IE175 protein and lacked the IE110 N-terminal domain that confers punctate characteristics. This hybrid IE175(N)/IE110(C) protein gave an irregular nuclear diffuse pattern on its own but was redistributed very efficiently into spherical punctate granules after cotransfection with the wild-type HSV-1 IE110 protein. Similar colocalization interactions occurred with internally deleted forms of IE110 that lacked the zinc finger region or large segments from the center of the protein, including both cytoplasmic and elongated punctate forms, but C-terminal truncated versions of IE110 did not interact. In all such interactions, the punctate phenotype was dominant. Evidence that C-terminal segments of IE110 could also form stable mixed-subunit oligomers in vitro was obtained by coimmunoprecipitation of in vitro-translated IE110 polypeptides with different-size hemagglutinin epitope-tagged forms of the protein. This occurred only when the two forms were cotranslated, not when they were simply mixed together. An in vitro-synthesized IE110 C-terminal polypeptide also gave immunoprecipitable homodimers and heterodimers when two different-size forms were cross-linked with glutaraldehyde and reacted specifically with a bacterial glutathione *S*-transferase/IE110 C-terminal protein in far-Western blotting experiments. The use of various N-terminal and C-terminal truncated forms of IE110 in the in vivo assays revealed that the outer boundaries of the interaction domain mapped between codons 617 and 711, although inclusion of adjacent codons on either side increased the efficiency severalfold in some assays. We conclude that the C-terminal region of IE110 contains a high-affinity self-interaction domain that leads to stable dimer and higher-order complex formation both in DNA-transfected cells and in in vitro assays. This segment of IE110 is highly conserved between HSV-1 and HSV-2 and appears to have the potential to play an important role in the interaction with the IE175 protein, as well as in correct intracellular localization, but it is not present in the equivalent proteins from varicella-zoster virus, pseudorabies virus, or equine abortion virus.

The IE110 (ICP0) protein of herpes simplex virus type 1 (HSV-1) is one of several nuclear phosphorylated proteins that are synthesized during the first few hours after infection and are thought to play an important role in transcriptional regulation. Unlike IE175 (ICP4), the IE110 gene product is not essential for lytic cycle productive infection when input virion components are present (50, 51), but it does appear to be an absolute requirement when infection is accomplished with purified viral DNA (3). On the other hand, an intact IE110 gene appears to be both necessary to trigger reactivation from the latent state in animal models and sufficient to trigger reactivation in cell culture model systems (26, 32, 49, 56). Therefore, the suspicion has grown that IE110 may have at least two roles, first as an accessory regulatory protein for efficient completion of lytic cycle gene expression (5, 8, 51), and second as the initiator of an alternative pathway leading to lytic cycle expression in the absence of VP16 during reactivation from the quiescent latent state in sensory neurons (3, 26, 28, 32, 44, 49, 56).

IE110 is translated from a spliced 2.7-kb mRNA containing three exons (45, 55) under the transcriptional control of a large complex upstream enhancer region encompassing multiple octamer/TAATGARAT-type Oct-1 binding sites and VP16 response elements (1, 45). The predicted protein coding region includes several consensus casein kinase II sites at the N terminus of exon 2 and a novel Cys-rich double zinc finger domain in the center of exon 2, together with two 50- to 70-amino-acid Pro-rich domains and a Ser-Ala-rich repeat region in exon 3 (45). The equivalent proteins in varicella-zoster virus, pseudorabies virus, and equine abortion virus share only the Cys-rich zinc finger cluster (30% homology over 75 amino acids), and the varicella-zoster virus version (gene 61) has been described as a transcriptional repressor in certain cell types (39). However, the HSV-1 and HSV-2 IE110 proteins possess much more extensive homology compared with other members of the group, particularly in two contiguous domains of 130 to 140 amino acids each, one in exon 2 (region II) and the other at the C terminus of exon 3 (region V), which are between 80 and 85% identical in the two HSV subtypes (35).

The intact IE110 gene is expressed efficiently as an isolated

* Corresponding author. Mailing address: The Virology Laboratories, Department of Pharmacology and Molecular Sciences, Johns Hopkins University School of Medicine, 725 N. Wolfe St., Baltimore, MD 21205. Phone: (410) 955-8686. Fax: (410) 955-8685.

† Present address: Medical College of Wisconsin, Milwaukee, WI 53226.

genomic DNA clone in transient DNA transfection assays, yielding a single known phosphorylated protein product with apparent molecular mass of 110 kDa (despite a predicted unmodified size of 85 kDa). This protein normally localizes in a very unusual punctate pattern consisting of several dozen phase-dense granules with smooth spherical profiles distributed throughout the nucleus in DNA-transfected cells (9, 11, 16, 22, 23, 38) and in a much smaller micropunctate pattern at early times in infected cells (28a, 29). In other studies, we have mapped this characteristic to within the N-terminal 245 amino acids of the 775-amino-acid protein and found that even after deletion of the nuclear localization signal at codons 501 to 506, the IE110 protein retains this distinctive punctate distribution within the cytoplasm (25, 38). In contrast, the HSV IE175 protein produces a uniform diffuse distribution pattern in the nuclei of transfected cells. However, cotransfection of the IE175 gene together with the IE110 gene into the same cells leads to colocalization of some of the newly expressed IE175 protein product along with the IE110 protein in these punctate granules (25, 38). The minimal IE175-IE110 interaction domains that are responsible for this colocalization feature appear to map to the within C-terminal one-third of each protein (25, 37).

In transient cotransfection assays with chloramphenicol acetyltransferase reporter genes, the IE110 protein behaves as a nonspecific transactivator of heterologous promoters as well as HSV target promoters (14, 16, 17, 21, 41–44, 47). In some assays, IE110 and IE175 work synergistically to specifically boost expression from viral target promoters (9, 14, 17, 22, 47). The use of both deletion and insertion mutant forms of IE110 in such assays has revealed that the Cys-rich cluster in exon 2 is the most important domain in the protein for transactivation, although the C-terminal portion of exon 3 also plays a significant role, especially for synergism with cotransfected IE175 (8, 9, 16). In general, the results for reactivation efficiency also parallel the transactivation findings with regard to the critical role of the Cys-rich domain relative to other segments of the protein (56).

Although IE110 binds to DNA-cellulose columns (18, 27), no direct evidence for specific or nonspecific DNA binding properties in solution has been obtained as yet (18), and the mechanisms of transactivation and promoter targeting are unknown. Several recent reports have suggested that IE110 may dimerize or oligomerize, based on biochemical properties of the purified intact IE110 protein and dominant negative competitor effects of certain deletion mutants in functional assays (7, 18, 54). In this report, we describe evidence for subunit homodimerization interactions from colocalization in DNA-transfected cells. We have also used cross-linking, immunoprecipitation, and far-Western blotting studies with in vitro-translated polypeptides and *Escherichia coli* glutathione *S*-transferase (GST) fusion proteins to map a specific dimerization domain within the C-terminal segment of the HSV-1 IE110 protein. Wild-type and mutant forms of the HSV IE110 transactivator protein have been produced previously in adenovirus (58), baculovirus (18), and vaccinia virus (57) expression systems, as well as in transient transfection assays, but to our knowledge, neither *E. coli* nor in vitro transcription systems have been exploited previously to begin to study the biochemical properties of this protein.

(Some of these studies were included as part of the Ph.D. thesis of M.-A. Harrigan-Mullen [25].)

MATERIALS AND METHODS

IE110 expression vectors. The parent wild-type IE110 mammalian expression vectors used in DNA transfection experiments utilized either the cognate HSV-1(KOS) IE110 upstream promoter region (1) from position −800 to +123 (pGH92) or the simian cytomegalovirus (SCMV) (Colburn) IE94 upstream promoter/enhancer region from −990 to +30 (pGH94). In each case, the appropriate promoter region was placed directly in front of an HSV-1(KOS) DNA fragment derived from pIGA15 that contained the fully intact and functionally active genomic IE110 coding sequence, together with its leader, introns, and 3′ control elements from position +120 to approximately +5000 (21, 41, 48). The internally deleted cytoplasmic IE110(Δ365–518) in pMM63 was generated from pGH94 by insertion of a *Bcl*I-*Bgl*II-*Mlu*I linker followed by cleavage at the *Bgl*II site, filling in with Klenow DNA polymerase, and religation to create an in-frame junction. The other IE110 deletion and truncation mutants used, viz., IE110(Δ105–244) encoded by pMM68, IE110(Δ105–177) encoded by pMM72, IE110(Δ311–364) encoded by pGH215, IE110(Δ365–518) encoded by pMM63, IE110(Δ398–461) encoded by pMM1, IE110(*tm*365) encoded by pMM65, IE110(*tm*518) encoded by pMM74, IE110(*tm*711) encoded by pMM73, and IE110(*tm*767) encoded by pMM82, are all described in detail elsewhere (25, 38).

The IE175/IE110 hybrid gene construction. The in-frame joining of a 383-amino-acid N-terminal segment of IE175 to a 463-amino-acid C-terminal region from IE110 was accomplished by first inserting 12-mer *Bgl*II linkers both into the *Stu*I site at IE175 codon 383 in the SCMV/IE175 effector plasmid pGH114 (48) to create plasmid pMM12 and into the *Nru*I site at IE110 codon 312 in the SCMV/IE110 effector plasmid pGH94 to create pMM48. The isolated 5.5-kb *Eco*RI-*Bgl*II fragment from pMM12 and 2.3-kb *Eco*RI-*Bgl*II fragment from pMM48 were then ligated together to form pGH216, encoding the hybrid SCMV IE175(1–383)/IE110(313–775) protein.

In vitro transcription vectors for IE110 proteins. For synthesis of C-terminal segments of the HSV-1 IE110 protein by in vitro transcription-translation procedures, two principal versions of the IE110 coding region were ligated in frame behind the high-expression leader and initiator codon region from black beetle virus (BBV) described by Lieberman et al. (33) and Dasmahapatra (12). First, a set of *Bgl*II linker versions of the BBV leader region in all three reading frames in the pGEM background was constructed (pGH253, pGH254, and pGH255). Second, *Bgl*II linkers were also inserted into the *Mlu*I (pMM56) and *Sna*BI (pMM43) sites of pGH94. Finally, isolated 1.9- or 3.0-kb *Bgl*II-*Eco*RI fragments from pMM56 or pMM43 were inserted into the appropriate in-frame *Bgl*II sites in the BBV vector background to create BBV/IE110(518–775) in plasmid pGH326, which we refer to as IE110(3C), and BBV/IE110(245–775) in plasmid pGH327, which we refer to as IE110(exon3).

To generate a series of C-terminal truncations of the untagged IE110(exon3) and IE110(3C) proteins, the appropriate plasmids were linearized with various different enzymes before being transcribed by T7 polymerase (see legends to Fig. 5 and 6). Cleavage of pGH327 with *Not*I, *Mlu*I, *Aat*II, *Bst*EII, and *Sal*I generated IE110(exon3) truncations *tm*392, *tm*517, *tm*552, *tm*711, and *tm*767, respectively. Cleavage of pGH326 with *Sfi*I, *Xcm*I, *Bst*EII, *Pml*I, and *Sal*I generated IE110(3C) truncations *tm*615, *tm*669, *tm*711, *tm*714, and *tm*767, respectively.

Four N-terminally deleted versions of the untagged IE110(3C) protein were also constructed. First, a *Bgl*II linker was added to the T4 polymerase-blunted *Aat*II site in pGH92

to create pMM77a, and then an isolated 1.8-kb *Bgl*II-to-*Eco*RI fragment from pMM77 was inserted in frame into pGH253. The resulting plasmid pGH449 encodes BBV/IE110(555–775). Second, a 14-mer *Bgl*II linker was added to a 1.4-kb *Sfi*I fragment from pGH326 after blunting with T4 polymerase, and the 1.4-kb *Bgl*II-*Bgl*II fragment was inserted in frame into pGH253 to produce BBV/IE110(617–775) in pGH450. Third, a 14-bp *Bgl*II linker was added at the T4 polymerase-blunted *Xcm*I site in pGH326, and an 800-bp *Bgl*II-*Bgl*II fragment was inserted in-frame into pGH253 at the *Bgl*II site, creating pGH454 encoding BBV/IE110(671–775). Finally, a 10-bp *Bgl*II linker was inserted into pGH326 at the *E. coli* Klenow polymerase-filled-in *Bsi*WI site, and an isolated 1.2-kb *Bgl*II-*Eco*RI fragment was then ligated in frame into pGH253 to create pGH463 encoding BBV/IE110(680–775).

HA epitope-tagged IE110 proteins. To add the influenza virus hemagglutinin (HA) epitope tag at the N terminus, a 36-mer oligonucleotide pair, LGH519/520, encoding amino acids YPYDVPDYA (19) bounded by *Bam*HI and *Bgl*II sites was inserted in frame as single or tandem repeat copies into BBV expression vectors. Insertion at the 5′ *Bam*HI sites in pGH326 and pGH327 generated pGH428 expressing an HA/IE110(3C) polypeptide, pGH429 for HA/IE110(exon3), pGH439 for HA_2/IE110(3C), and pGH440 for both HA_2/IE110(exon3) and HA_2/IE110(3N).

For addition of the HA epitope at the C terminus, 14-mer *Bgl*II linkers were first inserted at the *Sal*I sites of pGH326 and pGH327 (after blunt ending by the Klenow fill-in reaction) to generate pGH400 and pGH403. Single copies of the HA oligonucleotides were then added in frame at the modified *Sal*I sites (codon 768) to generate pGH423 expressing IE110(3C)/HA and pGH424 encoding IE110(exon3)/HA. For an expression vector version expressing IE110(1–767/HA_2), we first replaced a *Bsi*WI-to-*Eco*RI fragment in pGH92 with the equivalent *Bsi*WI-to-*Eco*RI fragment from pGH423 to give pGH498. Finally, a second 3′ HA tag oligonucleotide pair was inserted in frame at the *Bgl*II site adjacent to the first HA copy in pGH498 to create pGH521.

GST/IE110 fusion proteins produced in *E. coli*. Three different segments of HSV-1 IE110 were placed in frame behind the 26-kDa GST coding region in pGEX-3X plasmid vectors (Pharmacia). Initially, pGEX-3X containing a factor X cleavage site was converted to a set of derivatives containing *Bgl*II restriction sites added in all three reading frames at the *Sma*I site (pGH416, pGH417, and pGH418). IE110 codons 23 to 245 were amplified by PCR from pGH92 template DNA, using 5′ and 3′ primers containing added *Bam*HI-*Bgl*II-*Aat*II and *Bam*HI-*Bgl*II-*Sna*BI linker sites, and then inserted as a 700-bp *Bgl*II-*Bgl*II fragment into the *Bgl*II site in pGH417 to generate plasmid pGH426 encoding GST/IE110(exon 2). After addition of a 12-mer *Eco*RI linker at the filled-in *Aat*II site in pGH327, an N-terminal exon 3 segment containing IE110 codons 245 to 553 was moved as a 925-bp *Bgl*II-*Aat*II fragment into pGH418 to create plasmid pGH452 encoding GST/IE110(3N). The C-terminal segment of HSV-1 IE110 containing codons 518 to 775 was moved directly as a 1.9-kb *Bgl*II-*Eco*RI fragment from pGH326 into pGH417 to give plasmid pGH438 encoding GST/IE110(3C). These three fusion proteins were synthesized after isopropylthiogalactopyranoside (IPTG) induction of *E. coli* DH1 host cells and were expected to have molecular masses of 52, 63, and 56 kDa, respectively. However, the major soluble polypeptides recovered from the lysed cells after GST-Sepharose affinity purification ran in sodium dodecyl sulfate (SDS)-polyacrylamide gels as 64 kDa for GST/IE110(exon 2) and 57 kDa for GST/IE110(3C), whereas GST/IE110(3N) yielded a series of degraded fragments ranging in size from 25 to 35 kDa.

Similar pGEX-based plasmids harboring N-terminal (codons 1 to 163) and C-terminal (codons 168 to 339) segments of human TATAA-binding protein (TBP) as GST/TBP(N) and GST/TBP(C) were obtained from John Sinclair (University of Cambridge Clinical Center, Addenbrooke's Hospital, Cambridge, England) and were described previously by Hagemeier et al. (24).

Antisera. Ascites fluid containing anti-HA mouse monoclonal antibody (MAb) 12CA5 was obtained from Berkeley Antibody Co. and used undiluted for immunoprecipitation and at 1/150 dilution for indirect immunofluorescence assay (IFA). Rabbit polyclonal antipeptide antiserum (PAb) directed against the HSV-1 IE110 C-terminal amino acids 762-SGEQ GASTRDEGKQ-775 was generated by procedures described by Pizzorno et al. (46) after addition of Tyr at the N end and Ser-Cys at the C end of the peptide and conjugation to keyhole limpet hemocyanin. Confirmation of the specificity of this antibody for the C terminus of IE110 was obtained by transient transfection and IFA with a panel of deleted expression plasmids encoding variants of IE110 (see Fig. 2). Two similar rabbit antipeptide PAbs directed against the N termini of HSV-1 IE110 and HSV-1 IE175 and mapping of the location of the epitope for the 58S mouse MAb against IE175 are described elsewhere (25, 38). All PAbs were used undiluted for immunoprecipitation and diluted 1:350-fold for IFA.

Transient DNA transfection and IFA. Short-term DNA transfection of CsCl-purified plasmid DNA by the calcium phosphate-plus-glycerol shock procedure in *N*-2-hydroxyethylpiperazine-*N*′-2-ethanesulfonic acid (HEPES) buffer was carried out in Vero (African green monkey kidney fibroblasts) or 293 (human embryonic kidney fibroblasts transformed with adenovirus E1A and E1B) monolayers in two-well or four-well slide chambers as described by Middleton et al. (36) and LaFemina et al. (31). The cells were fixed with absolute methanol at −20°C at 40 h after DNA transfection and incubated with monoclonal or polyclonal antisera at 1:350-fold dilution followed by fluorescein isothiocyanate (FITC)-labeled goat anti-mouse or anti-rabbit immunoglobulin G (IgG) antibody at 1:100-fold dilution. For the double-label experiments shown in Fig. 1A, the slides were incubated in succession with rabbit anti-IE110(N) PAb and FITC-labeled goat anti-rabbit IgG and then either with mouse anti-HA MAb and goat anti-mouse IgG or with rabbit anti-IE175(N) PAb and rhodamine-labeled goat anti-rabbit IgG, with thorough washing steps between each antibody sample. Slides were screened and photographed with a 40× oil immersion objective on a Leitz epifluorescence microscope using Kodak T-MAX ASA 3200 film. In general, positive IFA results with the wild-type IE110 effector plasmid (pGH92 or pGH94) were obtained in between 3 to 10% of the transfected Vero cells in each culture and in 20 to 30% of transfected 293 cells.

In vitro transcription and translation. RNA samples were synthesized and capped in vitro from linearized plasmid DNA with T7 polymerase, using the Stratagene mCAP kit and protocols. For DNA linearized with 3′-overhanging cleavage sites, the ends were first repaired with T4 DNA polymerase. Approximately 1-μg samples of each RNA were then used for in vitro translation in rabbit reticulocyte lysates, using the Promega kit, reagents, and protocols, including 1 mCi of [^{35}S]methionine (1,000 Ci/mol) per ml.

Immunoprecipitation and cross-linking. Immunoprecipitation of HA-tagged proteins was done as recommended by Kolodziej and Young (30). Ten-microliter samples of in vitro-translated lysate proteins were diluted 40-fold into 20 mM

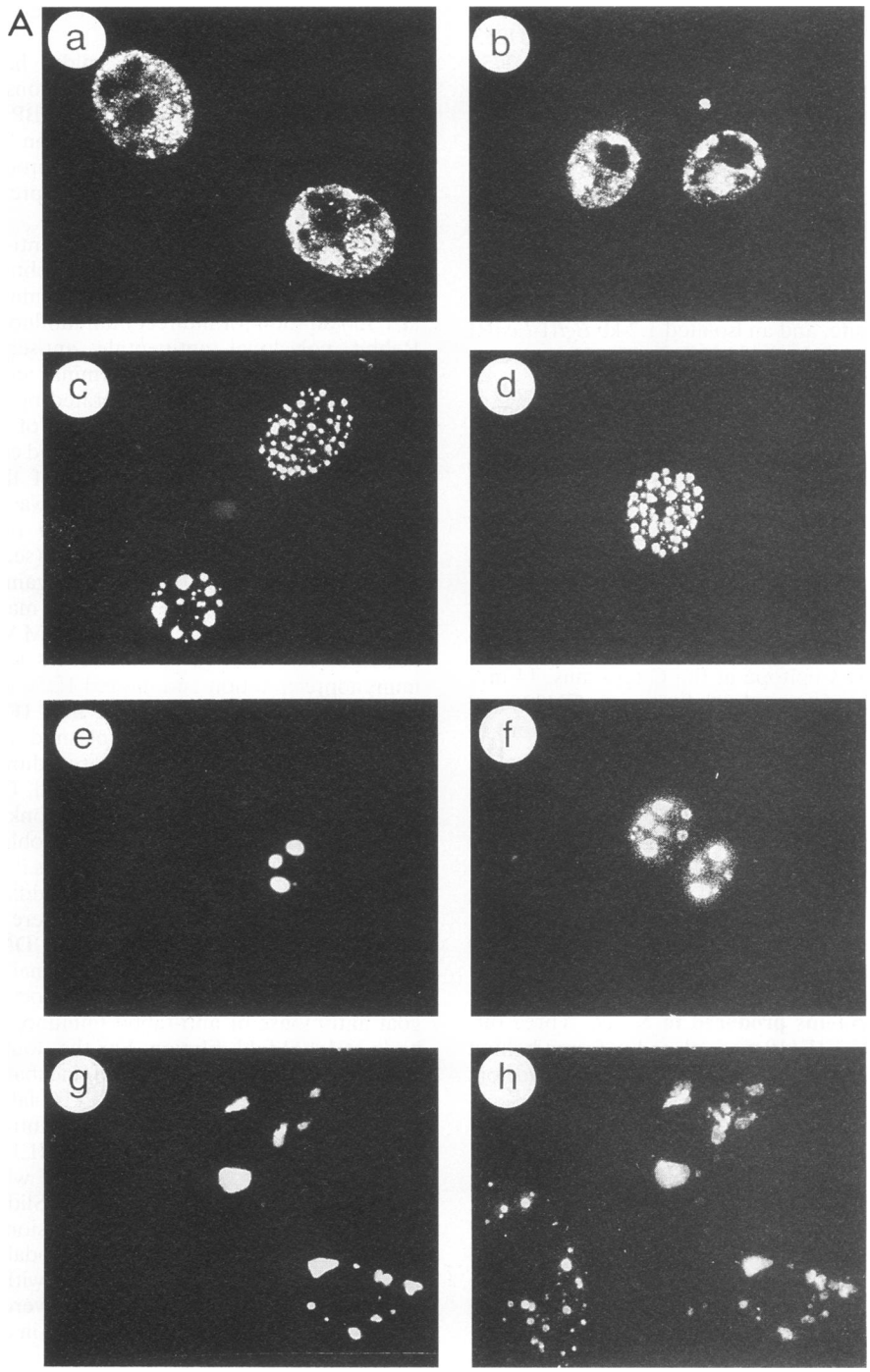

FIG. 1. Alteration of the intracellular localization pattern of a nonpunctate IE175(N)/IE110(C) hybrid protein in cells coexpressing various forms of the punctate IE110 protein. Plasmids encoding the IE175(1–383)/IE110(312–775) hybrid gene (in pGH216) either alone or in combination with plasmids encoding the wild-type IE110 gene or deletions were transfected into monolayer Vero or 293 cell cultures in a transient expression system. In most panels, the IE175/IE110 hybrid protein was detected by IFA with rabbit antipeptide PAb against the N terminus of IE175 and an FITC-labeled second antibody. (A) Vero cells. a and b, examples of the nuclear diffuse-plus-irregular clumps pattern obtained with the IE175-tagged IE110(C) hybrid protein alone in Vero cells. c and d, representative nuclear punctate patterns obtained with the hybrid protein (pGH216) after cotransfection with wild-type IE110 (pGH92). e and f, double-label IFA showing colocalization of the IE175/IE110 hybrid protein with a wild-type nuclear punctate form of IE110 containing a C-terminal HA tag. In panel e, the IE175/IE110 hybrid protein coexpressed in one of the cells was detected with rabbit anti-IE175 PAb and rhodamine-labeled goat anti-rabbit IgG. In panel f, the IE110(1–767/HA_2) protein encoded by pGH521 was detected within two cells in the same field by using mouse anti-HA MAb and FITC-labeled goat anti-mouse IgG. g and h, double-label IFA showing colocalization of the IE175/IE110 hybrid protein when cotransfected with the cytoplasmic punctate IE110(Δ365–518) protein encoded by pMM63. In panel g, the IE175/IE110 hybrid protein was detected within two coexpressing cells by using rabbit anti-IE175(N) PAb and rhodamine-labeled goat anti-rabbit IgG. In panel h, the IE110(Δ363–518) deletion protein was detected within three cells in the same field by using rabbit anti-IE110(N) PAb and FITC-labeled goat anti-rabbit IgG. Note that oneof the cells shown within each double-labeled pair

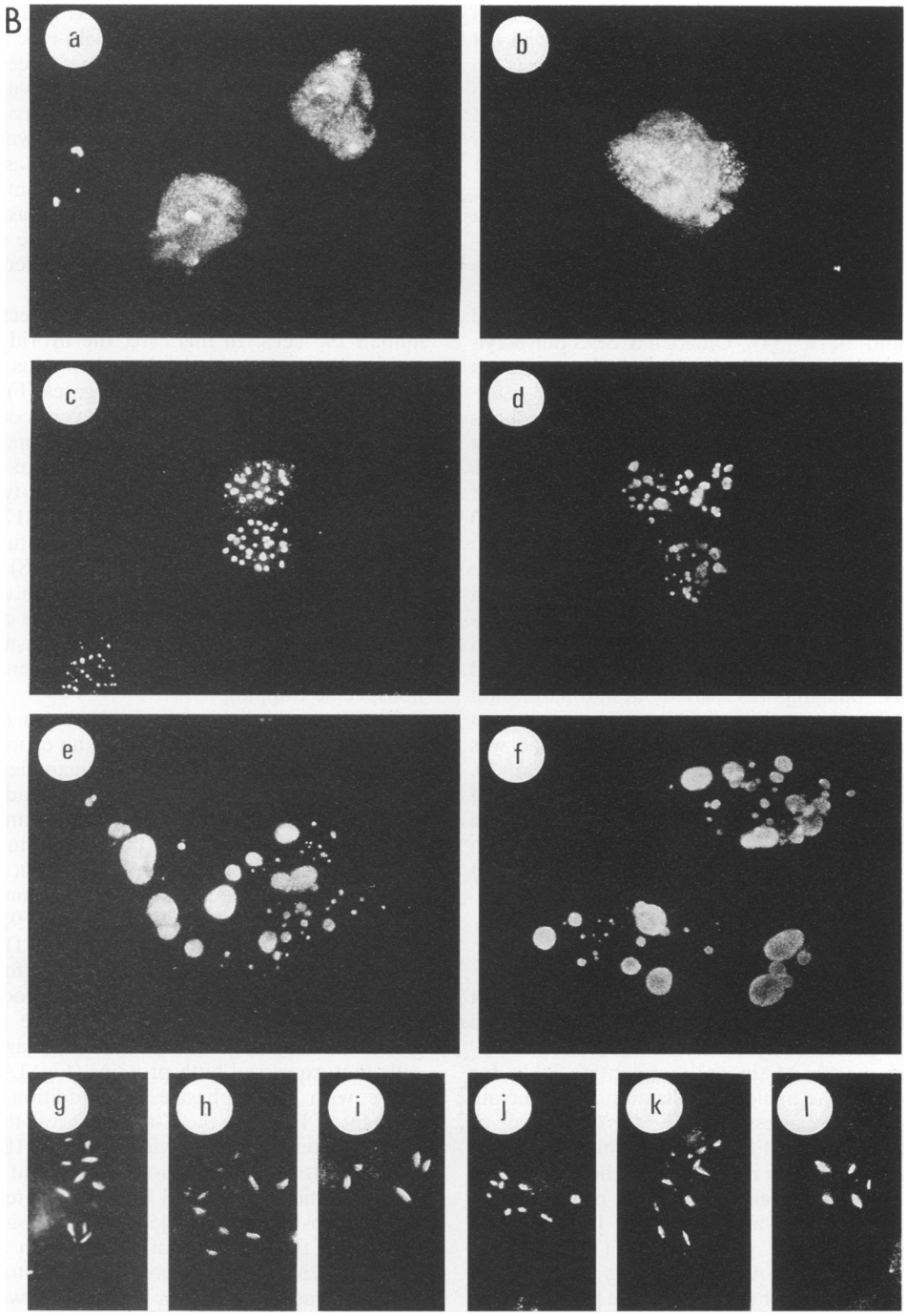

in panels e to h expressed IE110 only, which confirmed the absence of any cross-reactivitybetween the IE175(N) antibodies and the IE110 protein. (B) 293 cells. All panels except g to i show single-label detection of the IE175-tagged IE110(C) hybrid protein with rabbit IE175(N) PAb and FITC-labeled second antibody. a and b, typical examples of the uniform mixed nuclear-plus-cytoplasmic diffuse pattern obtained with the hybrid protein encoded by pGH216 when transfected alone. c and d, nuclear punctate patterns obtained with the hybrid protein after cotransfection with wild-type IE110 (pGH92). e and f, cytoplasmic punctate localization patterns of the hybrid protein after cotransfection with IE110(Δ365–518) encoded by plasmid pMM63. g to l, nuclear elongated punctate patterns of the hybrid protein obtained after cotransfection with a zinc finger-deleted form of IE110. g to i, control patterns of IE110(Δ105–244) from pMM68 alone detected with FITC-labeled anti-IE110(N) PAb. j to l, IE175(N)/IE110(C) hybrid protein from pGH216 cotransfected with IE110(Δ105–244) from pMM68 and detected with FITC anti-IE175(N) PAb.

HEPES buffer (pH 7.9) containing 10 mM EDTA, 10 mM dithiothreitol, 400 mM $(NH_4)_2SO_4$, 1% Triton, 0.1% SDS, and 10% glycerol, with phenylmethylsulfonyl fluoride or other protease inhibitors. The samples were then incubated with 1 μl of undiluted antibody for 1 h at 4°C and centrifuged at 14,000 × *g* for 15 min at 4°C. The supernatant was added to protein A-Sepharose beads (50 μl at 50 mg/ml; Pharmacia) and rocked gently at 4°C for another 30 min. The beads were washed and

pelleted three times in the same buffer, except for a final reduction to 50 mM $(NH_4)_2SO_4$, followed by boiling in gel loading buffer for storage or analysis by electrophoresis on SDS–9% polyacrylamide gels. For cross-linking, 10 μl of the in vitro-translated lysate was first diluted with 80 μl of 10 mM potassium phosphate buffer (pH 8.0), then mixed with 10 μl of 0.1% freshly diluted glutaraldehyde, and incubated for 1 h at 23°C (6, 40). In all immunoprecipitation experiments, the control untreated samples shown represent 10% of the amount originally incubated with antiserum. Quantitation of immunoprecipitated bands involved analysis of the autoradiographs with a Howtek-3 scanner and Millipore BioImage software.

Far-Western blotting. The procedure used was adapted from Lieberman and Berk (34). Unlabeled SDS-polyacrylamide gel-fractionated proteins (approximately 5 μg of each GST fusion protein per lane) were transferred to a nitrocellulose membrane sheet (6 by 6 in. [15 by 15 cm]) by electroblotting in Tris-glycine buffer with 20% methanol at 30 V overnight in a Bio-Rad Trans-Blot apparatus (53). Proteins on the membrane were denatured by shaking at 23°C in 100 ml of renaturation buffer (20 mM HEPES [pH 7.9], 10% glycerol, 60 mM KCl, 6 mM $MgCl_2$, 0.6 mM EDTA, 10 mM dithiothreitol) containing 6 M guanidine HCl for 30 min. To renature the proteins, the membrane was incubated first in renaturation buffer containing 100 mM guanidine HCl and 0.02% polyvinylpyrrolidone–0.02% Ficoll (PVP-F) for 2 h and then in buffer containing 100 mM guanidine HCl, 0.3% Tween 20, and 0.02% PVP-F for 2 h. Blocking was carried out in renaturation buffer containing 0.3% Tween 20 and 50 mg of bovine serum albumin (BSA) per ml for 1 h. Finally, the membrane was incubated in renaturation buffer containing 0.3% Tween 20, 0.02% PVP-F, 0.02% BSA, plus 50 μl (10,000 cpm) of [^{35}S]Met-labeled in vitro-translated protein probe at room temperature for 16 h. Washing was accomplished by two 10-min shaking steps in 20 mM HEPES (pH 7.9)–100 mM KCl–6 mM $MgCl_2$–0.2 mM EDTA–10 mM dithiothreitol.

RESULTS

Influence of IE110 on the intracellular distribution of a cotransfected IE110/IE175 hybrid protein. We have described elsewhere the use of panels of hybrid IE110/IE175 and IE175/IE110 proteins and specific MAbs and antipeptide PAbs for analysis and mapping of the nuclear localization and punctate characteristics in transient expression assays (38). One type of hybrid gene, in which the IE110 N-terminal domain encoding the punctate characteristics was replaced with the N terminus of IE175 as the equivalent of an epitope tag, proved useful here for examining IE110 self-interactions by IFA. Plasmid pGH216 encoding the hybrid protein IE175(1–353)/IE110 (313–775) (Fig. 2A) gave an IFA pattern on its own in Vero cells consisting predominantly of uniform diffuse products plus large irregular patches in the nucleus (Fig. 1A, panels a and b). In addition, 20 to 25% of the positive cells harbored large cytoplasmic aggregates as well (not shown). The pattern was exactly the same whether the protein product of pGH216 was detected with the IE175(N) PAb directed against the N terminus of IE175 or with the IE110(C) PAb directed against the extreme C terminus of IE110, indicating that the expected full-length hybrid protein was synthesized from this construction (Fig. 2A).

Surprisingly, when the pGH216 IE175(N)/IE110(C) expression plasmid was cotransfected into Vero cells together with an intact wild-type IE110 expression plasmid (either pGH92 or pGH94), the hybrid polypeptide product detected with the IE175(N) PAb was now redistributed predominantly as crisply defined nuclear punctate granules (Fig. 1A, panels c and d) of the type typically formed by the wild-type IE110 protein alone (11, 38). Most of the immunofluorescence associated with the hybrid protein colocalized precisely with the phase-dense IE110-associated nuclear granules observed in the same cells by phase-contrast microscopy (not shown). The efficiency of expression of the hybrid protein from plasmid pGH216 on its own was considerably lower than that from either of the parent wild-type IE175 or IE110 effector plasmid (pGH114 and pGH92), but the number of IFA-positive cells was boosted 5- to 10-fold in the presence of the cotransfected wild-type IE110 transactivator protein.

We also carried out similar cotransfection experiments in human 293 cells. In this case, the hybrid protein on its own gave a more typical mixed nuclear plus cytoplasmic diffuse pattern without the patchy aggregates (Fig. 1B, panels a and b). Nevertheless, again virtually every cotransfected 293 cell that was positive for the IE175 epitope in the IE175(N)/IE110(C) hybrid protein expressed it in a nuclear punctate pattern when cotransfected with the wild-type IE110 gene (Fig. 1B, panels c and d). Note that the IE175(N)-terminal PAb used here does not cross-react at all with wild-type IE110 or cellular proteins in IFA experiments (38) (Table 1). Furthermore, cotransfection with IE110 has no effect on the diffuse nuclear distribution of a control human cytomegalovirus IE1 protein expressed similarly from a plasmid DNA vector in Vero cells (38). Therefore, the phenomenon does not involve nonspecific trapping.

To carry out the cotransfection as a double-label experiment, we first needed to construct an expression vector encoding a form of IE110 that could be unambiguously distinguished from the hybrid protein. Therefore, we added two copies of a synthetic oligonucleotide pair encoding an influenza virus HA epitope at the *Sal*I site near the C terminus of wild-type IE110 in the pGH92 background. This IE110(1–767/HA_2) protein was found to localize in typical nuclear punctate granules when detected with a mouse anti-HA MAb (19) followed by FITC-labeled anti-mouse IgG (Fig. 1A, panel f). Furthermore after cotransfection, the redistributed pattern for the hybrid protein detected with anti-IE175(N) PAb and rhodamine-labeled anti-rabbit IgG exactly coincided within the pattern of punctate granules containing the wild-type HA-tagged IE110 in those cells that expressed both proteins (Fig. 1A, panel e).

We wish to emphasize that addition of the N-terminal segment of IE175 to the C-terminal two-thirds of IE110 in the hybrid protein simply provided both an IE175(N) epitope tag and a way to express a form of IE110 that lacked the punctate feature, which is encoded by IE110 N-terminal amino acids between positions 1 and 245 (38). Nonfusion versions of IE175 containing this segment of IE175, such as IE175(1–353) or IE175(1–823), gave uniform diffuse cytoplasmic or nuclear IFA patterns on their own (38) and showed no interaction at all when cotransfected with IE110 in these types of experiments (25, 37). Although we have shown elsewhere that the intact IE175 protein also colocalizes with IE110 in punctate granules in cotransfection experiments (38), the IE175-IE110 interaction function is far less efficient and has been mapped toward the C terminus of IE175 (25, 37), which was not present in the hybrid gene construction used here. Furthermore, that interaction can be detected only in Vero cells and not in 293 cells (37), in distinct contrast to the IE110 self-interaction demonstrated here.

Colocalization of the hybrid protein with a cytoplasmic punctate form of IE110. In a second set of experiments of this type, the hybrid IE175(1–353)/IE110(313–775) gene in pGH216 was cotransfected with a deleted form of the IE110

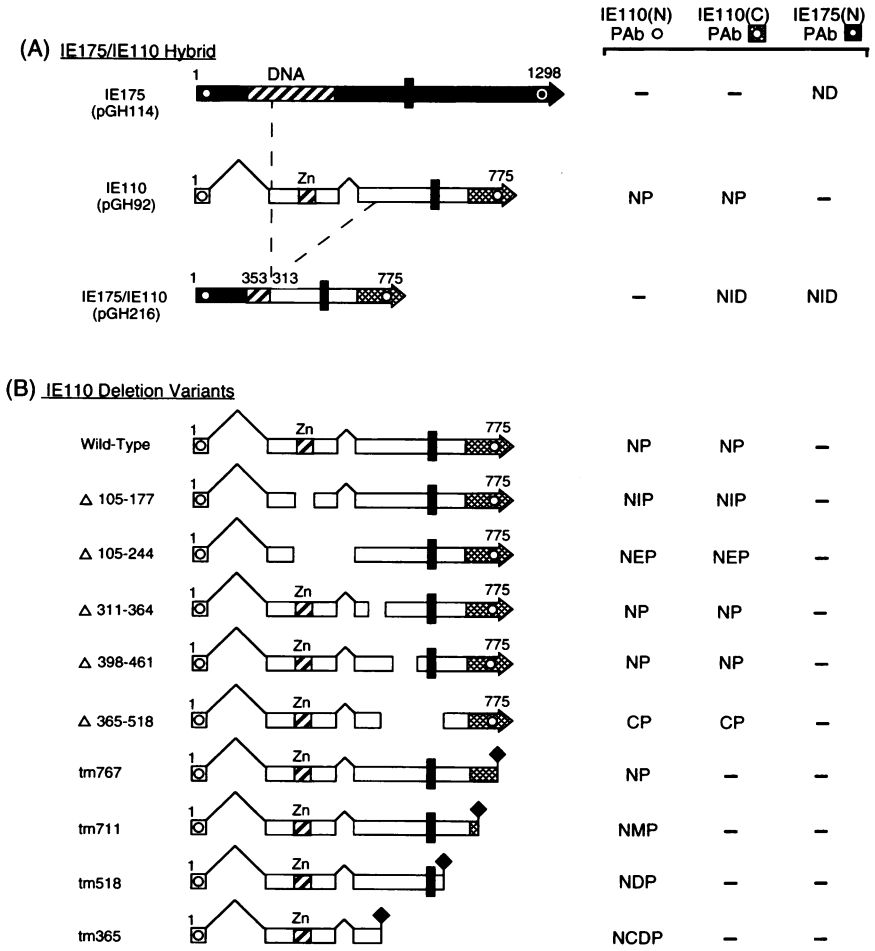

FIG. 2. Summary of the structures, epitope mapping, and intracellular localization of the IE175(N)/IE110(C) hybrid protein and of deletion and truncation variants of IE110. (A) Diagram illustrating the derivation of the hybrid IE175/IE110 test protein encoded in plasmid pGH216 relative to characteristic features of the parent wild-type HSV-1 IE175(ICP4) and spliced IE110(ICP0) mRNAs and proteins encoded by effector plasmids pGH114 and pGH92 (or pGH94), respectively. (B) Diagram comparing the structures of the series of truncated and deleted variants of IE110 used here. All are encoded in either the pGH92 (wild type) or pGH94 (SCMV/enhancer) expression vector background. In both diagrams, IE175 coding sequences are shown as a solid bar and arrowhead and IE110 coding sequences are shown as an open bar and arrowhead. Hatched bars denote the DNA-binding domain in IE175, the novel Cys-rich zinc finger cluster in IE110, and the highly conserved C-terminal domain V of HSV IE110. The known nuclear localization signals are shown as solid vertical bars. The mapped locations of the three N- and C-terminal rabbit PAb epitopes and the 58S anti-IE175 mouse MAb epitope that react with the antibodies used here (25, 38) are indicated by the open circles and a solid circle, respectively. Domain boundaries are defined by the HSV-1 codon numbers. The predominant intracellular distribution pattern of each polypeptide as detected by IFA with the IE110(N), IE110(C), or IE175(N) rabbit PAb is listed as an appropriate combination of nuclear (N), cytoplasmic (C), diffuse (D), punctate (P), micropunctate (MP), irregular punctate (IP), elongated punctate (EP), or irregular diffuse clumps (ID).

protein referred to as IE110(Δ364–518), which lacks the nuclear localization signal motif at codons 501 to 506 (25, 38) (Fig. 2B) and localizes predominantly in the cytoplasm (Fig. 1A, panel g). This time, the IE175 marker antibody again revealed a redistribution of the hybrid protein into a predominantly punctate pattern, except that it was now localized almost exclusively in the cytoplasm in both Vero cells (Fig. 1A, panel g) and 293 cells (Fig. 1B, panels e and f). In some control experiments, especially in 293 cells, the large overexpressed IE110(Δ364–518) cytoplasmic punctate granules could be detected as a dull cross-reacting autofluorescence under FITC conditions, even when the cells were stained with IE175 rabbit PAb or other nonrelevant antibodies, but this effect could be readily distinguished from the bright specific immunofluorescence obtained in those cells that also expressed the hybrid protein. This type of complication did not occur with any of the nuclear forms of IE110. However, when rhodamine-conjugated IE175 antibody was used in a double-label IFA experiment in Vero cells, the signals could be clearly distinguished (Fig. 1A, panels g and h). Importantly, this result showed not only that the IE175(N)/IE110(C) hybrid protein redistributed predominantly into cytoplasmic IE110-like punctate granules after cotransfection but also that these punctate granules were the same ones that contained the FITC-labeled IE110 protein (Fig. 1A, panel h).

Mapping of a domain within IE110 that is required for colocalization. The cotransfection analysis was also extended in both Vero and 293 cells to a series of eight additional deletion and truncation variants of IE110 (Fig. 2B), which produce several different and characteristic types of nuclear punctate or micropunctate products (38). As summarized in Table 1, the hybrid protein detected with the IE175(N) PAb

TABLE 1. Changes in the intracellular localization of the hybrid IE175/IE110 protein when cotransfected with deleted variants of the IE110 protein

Gene(s) involved	Plasmid(s) used	Immunofluorescence pattern[a]				Interaction[b]	
		Anti-IE110(N)		Anti-IE175(N)		Vero	293
		Vero	293	Vero	293		
IE175/IE110	pGH216	—	—	NID[c]	NCD		
IE110 wild type	pGH92	NP	NP	—	—		
	pGH92 + pGH216	NP	NP	NP	NP	+++	+++
IE110(Δ105–177)	pMM72	NP	NIP	—	—		
	pMM72 + pGH216	NP	NIP	NP	NIP	+++	+++
IE110(Δ105–244)	pMM68	NP	NEP	—	—		
	pMM68 + pGH216	NP	NEP	NP	NEP	+++	+++
IE110(Δ311–364)	pGH215	NP		—			
	pGH215 + pGH216	NP		NP		+++	
IE110(Δ398–461)	pMM1	NP		—			
	pMM1 + pGH216	NP		NP		+++	
IE110(Δ364–518)	pMM63	CP	CP	—	—		
	pMM63 + pGH216	CP	CP	CP	CP	+++	+++
IE110(*tm*767)	pMM82	NP		—			
	pMM82 + pGH216	NP		NP		+++	
IE110(*tm*711)	pMM73	NMP	NMP	—	—		
	pMM73 + pGH216	NMP (ND)[d]	NMP	NID[c] (ND)[d]	NCD (NMP)[d]	+/−	+/−
IE110(*tm*518)	pMM74	NDP	ND	—	—		
	pMM74 + pGH216	NDP	ND	NID[c]	NCD	—	?[e]
IE110(*tm*365)	pMM65	NCDP		—			
	pMM65 + pGH216	NCDP		NID[c]		—	

[a] NP, nuclear punctate; CP, cytoplasmic punctate; ND, nuclear diffuse; NID, nuclear diffuse with irregular large aggregates; NCD, nuclear and cytoplasmic diffuse; NIP, nuclear irregular punctate; NEP, nuclear elongated punctate; NMP, nuclear micropunctate; NDP, nuclear uniform diffuse with some micropunctate; NCDP, nuclear and cytoplasmic diffuse with punctate; —, not detectable.

[b] +++, 70 to 100% positive cells; ++, 40 to 70%; +, 10 to 35%; +/−, approximately 2 to 10%; —, less than 2%. In each case, at least 50 positive cells were scored.

[c] Includes cytoplasmic forms in 20 to 30% of the cells also.

[d] Only 5 to 10% of the positive cells showed the distribution pattern given in parentheses.

[e] Forms could not be distinguished sufficiently.

produced efficient colocalization interactions with IE110 (Δ105–177), IE110(Δ105–244), IE110(Δ311–364), IE110 (Δ398–461), and IE110(*tm*767). Again the redistribution was very dramatic (especially in 293 cells), with virtually all of the hybrid protein being detected in a punctate pattern of the same characteristic subtype as that shown by the particular cotransfected IE110 variant used.

Representative IFA patterns obtained after cotransfection with IE110(Δ105–244), which frequently gives an elongated punctate pattern in 293 cells on its own, are shown to illustrate this effect (Fig. 1B, panels g to l). In contrast, no obvious colocalization was observed with either the IE110(*tm*365) or IE110(*tm*518) species, both of which lack large sections from the C terminus of IE110 (Fig. 2B). Cotransfection with IE110(*tm*711), which displays a nuclear micropunctate pattern on its own, was considered inconclusive because only 5 to 10% of the cells produced a redistributed pattern with the hybrid protein (Table 1). When the IE110(N) PAb was used for IFA, there was little indication of a redistribution of any of the IE110 protein variants to colocalize with the hybrid protein, except perhaps with IE110(*tm*711).

These results confirmed not only that the IE110 protein was responsible for the change in location of the hybrid IE175(N)/IE110(C) protein but also that it was also able to drag the hybrid protein into whatever cellular compartment or subtype of punctate structure that the nonfusion version of IE110 occupied. Therefore, the IE110 protein appears to display a very strong self-association feature in DNA-transfected cells, and this property requires a segment of the protein encompassing an amino acid domain mapping between codons 518 and 767. Furthermore, both nuclear and cytoplasmic versions of wild-type IE110 displaying the punctate characteristics were always dominant over the nonpunctate hybrid IE175(N)/IE110(C) protein in the presumed hetero-oligomeric complexes.

Detection of heterodimer formation by immunoprecipitation of in vitro-translated proteins. The IFA results described above for cotransfected cells implied that two different forms of the IE110 protein could colocalize within the intracellular environment, presumably because of an ability to interact with one another by either direct or indirect means. To examine whether the existence of a direct high-affinity oligomerization motif within IE110 could be confirmed in vitro, we prepared three different-size forms of ^{35}S-labeled IE110 exon 3 in an appropriate plasmid vector for synthesis of [^{35}S]Met-labeled proteins by in vitro transcription and translation procedures (Fig. 3B). The largest forms, containing codons 245 to 775, gave 68-kDa polypeptides referred to as IE110(exon3) and the smallest forms, containing codons 518 to 775, gave 36-kDa polypeptides referred to as IE110(3C). A third 40-kDa form referred to as IE110(3N) was prepared by linearization of an intact exon 3 template at the *Mlu*I site (codon 518). To be able to immunoprecipitate these proteins, the influenza virus HA epitope was inserted in frame into some of these vectors, and we also prepared a new rabbit antipeptide PAb against codons 762 to 775 at the C terminus of IE110. The in vitro-translated ^{35}S-labeled versions of these IE110 polypeptides with either one or two copies of the HA epitope at the N terminus or at position 767 near the C terminus gave slightly different and reduced mobilities relative to the parent untagged forms in SDS-polyacrylamide gel electrophoresis. The identity of each species was confirmed by its ability to be immunoprecipitated

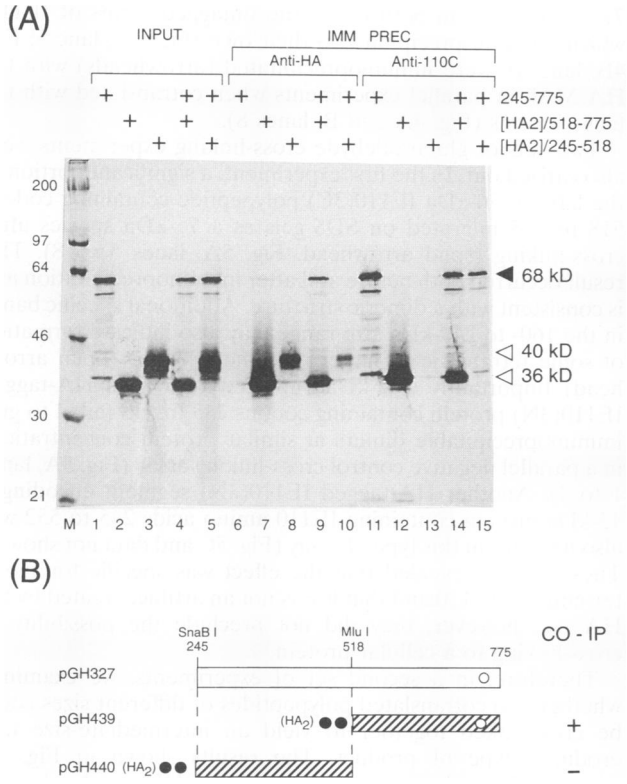

FIG. 3. Coimmunoprecipitation of tagged and untagged forms of IE110. (A) [^{35}S]Met-labeled IE110 proteins were synthesized in reticulocyte extracts from in vitro-transcribed RNA and analyzed by SDS-polyacrylamide gel electrophoresis with or without immunoprecipitation (IMM PREC). All template plasmid DNA samples were linearized with *Eco*RI or *Mlu*I before incubation with T7 RNA polymerase. Lanes: M, ^{14}C-labeled marker proteins; 1, 6, and 11, 68-kDa untagged IE110(exon3) from pGH327 (◀); 2, 7, and 12, 36-kDa HA_2/IE110(3C) from pGH439 (◁); 3, 8, and 13, 40-kDa HA_2/IE110(3N) from pGH440 linearized with *Mlu*I (◁); 4, 9, and 14, cotranslation of untagged IE110(exon3) plus HA_2/IE110(3C); 5, 10, and 15, cotranslation of untagged IE110(exon3) plus HA_2/IE110(3N); 1 to 5, input untreated proteins; 6 to 10, proteins recovered from immunoprecipitation with anti-HA mouse MAb; 11 to 15, proteins recovered from immunoprecipitation with anti-IE110(C) rabbit PAb. (B) Diagram illustrating the structures of the polypeptides involved. Hatched bars indicate epitope-tagged forms. Solid circles denote the positions of the HA epitope tags, and open circles indicate the IE110(C) PAb epitope. CO-IP, coimmunoprecipitation.

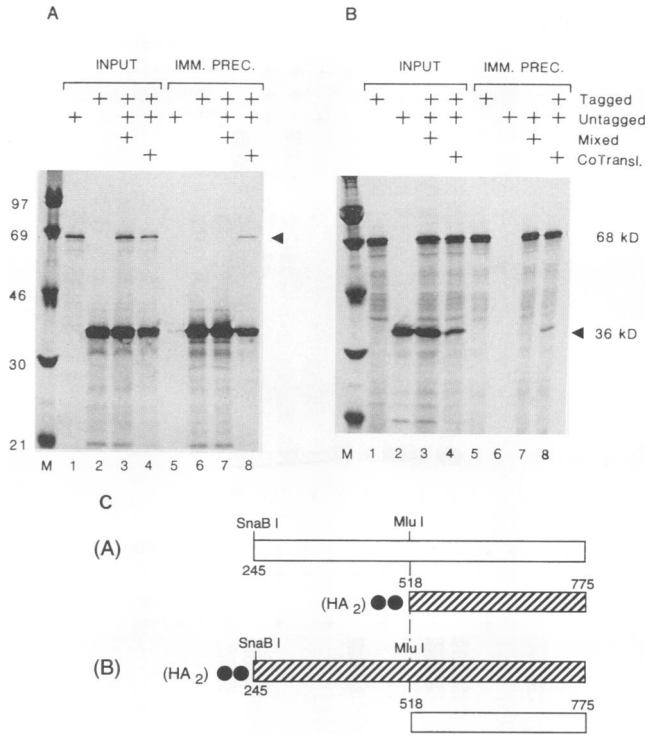

FIG. 4. Stable oligomeric subunit interactions require cotranslation. Immunoprecipitation (IMM. PREC.) experiments were carried out with either admixed or cotranslated (CoTransl.) [^{35}S]Met-labeled in vitro-translated proteins. In panels A and B, lanes 1 to 4 represent input untreated samples and lanes 5 to 8 represent proteins recovered from immunoprecipitation with HA MAb. (A) Lanes: M, ^{14}C-labeled size marker proteins; 1 and 5, untagged IE110(exon3) from pGH327(*Eco*RI); 2 and 6, HA_2/IE110(3C) from pGH439(*Eco*RI); 3 and 7, mixture of singly translated IE110(exon3) and HA_2/IE110(3C); 4 and 8, cotranslation of IE110(exon3) plus HA_2/IE110(3C). (B) Lanes: 1 and 5, HA_2/IE110(exon3) from plasmid pGH440(*Eco*RI); 2 and 6, untagged IE110(3C) from plasmid pGH326(*Eco*RI); 3 and 7, mixture of singly translated HA_2/IE110(exon3) and IE110(3C); 4 and 8, cotranslation of HA_2/IE110(exon3) and IE110(3C). Arrowheads denote the positions of coprecipitated untagged 68-kDa IE110(exon3) in panel A and 36-kDa IE110(3C) in panel B. (C) Diagram illustrating the structure of the polypeptides used in panels A and B. Hatched bars and solid circles denote epitope-tagged forms.

in the presence of the appropriate antibody but not by staphylococcal protein A-Sepharose beads alone.

In the first experiment shown, we examined whether an untagged form of intact 68-kDa IE110(exon3) protein could be coprecipitated when cotranslated with the smaller HA-tagged form of IE110(3C) or IE110(3N). Initial controls confirmed that the singly translated HA-tagged form of IE110(3C) was efficiently immunoprecipitated by both the HA MAb and the IE110(C) PAb (Fig. 3A, lanes 7 and 12), whereas parallel samples of the untagged IE110(exon 3) protein and HA-tagged IE110(N) protein were each specifically immunoprecipitated with only one, but not the other, of the HA MAb and the IE110(C) PAb reagents (Fig. 3A, lanes 6 and 11 compared with lanes 8 and 13). However, when the 68-kDa untagged IE110(exon3) protein was cotranslated with the 36-kDa HA/IE110(3C) protein, it was also efficiently immunoprecipitated with the HA antibody (solid arrowhead, Fig. 3A, lane 9). In contrast, cotranslation of the untagged IE110(exon3) protein with the 40-kDa HA/IE110(3N) protein failed to yield either an HA-coprecipitated IE110(exon3) band or an IE110(C)-coprecipitated HA/IE110(3N) band under similar conditions (Fig. 3A, lanes 10 and 15). These results provided strong evidence in support of a direct and specific protein-protein interaction that could be detected in vitro and allowed us to conclude that a functional oligomerization domain maps within the C-terminal half of exon 3 but not within the N-terminal half of exon 3 (Fig. 3B).

Subunit interactions in heterodimer cross-linking and mixing experiments. Additional evidence that the ability to coimmunoprecipitate represents folding of individual subunits into stable dimers or oligomers came from comparing the effect of simply mixing the two proteins rather than preparing them by cotranslation. Significantly, no interaction could be detected with mixtures of either the IE110(245–775) and HA_2/IE110(518–775) or the HA_2/IE110(245–775) and IE110(518–775) in vitro-translated protein samples (Fig. 4A and B, lanes

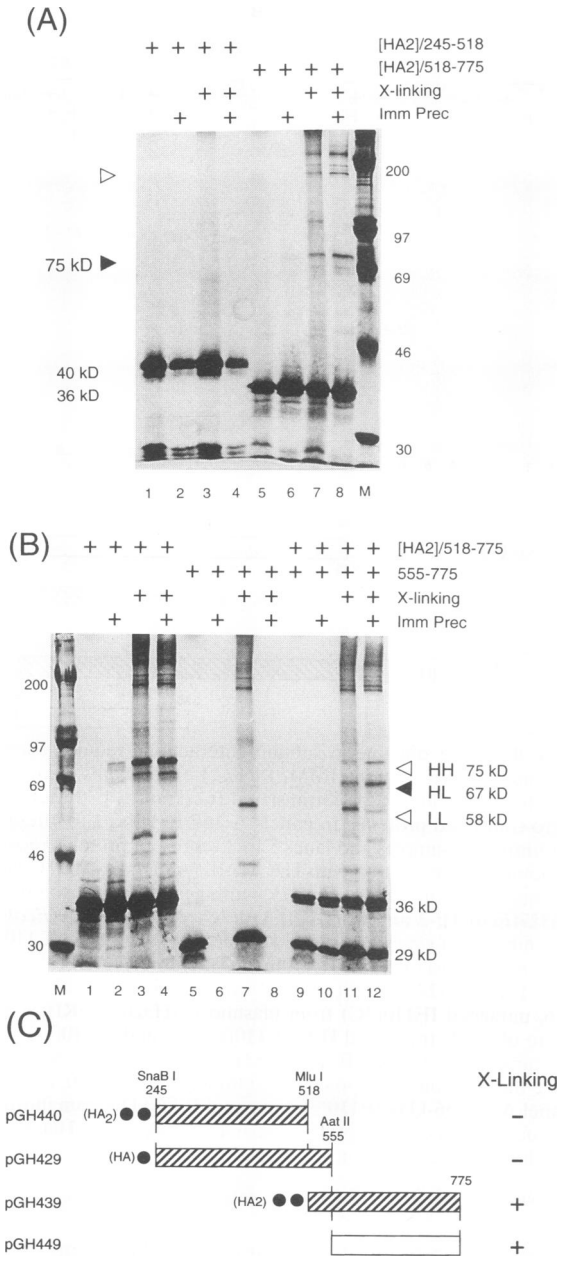

FIG. 5. Cross-linking and heterodimer formation by in vitro-translated IE110 proteins. (A) Cross-linking (X-linking) of IE110(3C) but not IE110(3N). Lanes: 1 to 4, HA_2/IE110(245–518) from pGH440 linearized with *Mlu*I; 5 to 8, HA_2/IE110(518–775) from *Eco*RI-linearized pGH439; 1 and 5, input ^{35}S-labeled protein; 2 and 6, HA MAb immunoprecipitation (Imm Prec) without cross-linking; 3 and 7, glutaraldehyde cross-linked samples without immunoprecipitation; 4 and 8, glutaraldehyde cross-linked samples after HA MAb immunoprecipitation; M, ^{14}C-labeled protein size markers. ◀, position of the major 75-kDa dimeric form of HA_2/IE110(518–775); ◁, possible multimeric forms. (B) Heterodimer formation between two different-size forms of IE110(3C). Lanes: 1 to 4, HA_2/IE110(518–775) from *Eco*RI-linearized pGH439; 5 to 8, untagged IE110(555–775) from *Eco*RI-linearized pGH449; 9 to 12, cotranslation of HA_2/IE110(518–775) and untagged IE110(555–775); 1, 5, and 9, input ^{35}S-labeled protein; 2, 6, and 10, HA MAb immunoprecipitation without cross-linking; 3, 7, and 11, glutaraldehyde cross-linked samples without immunoprecipitation; 4, 8, and 12, glutaraldehyde cross-linked samples after HA MAb immunoprecipitation; M, ^{14}C-labeled protein size markers. HH (◁), HL (◀), and LL (◁) denote expected positions of the large homodimer, heterodimer, and small homodimer forms, respectively. (C) Diagram illustrating the structures of the polypeptides used. Hatched bars denote epitope-tagged forms. Results for HA/IE110(245–555) are included but not shown in panels A and B.

7). In contrast, in both cases, the untagged forms of IE110, which failed to precipitate on their own (Fig. 4A, lane 5; Fig. 4B, lane 6), were immunoprecipitated (arrowheads) with the HA MAb in parallel experiments when cotranslated with the tagged forms (Fig. 4A and B, lanes 8).

Two sets of glutaraldehyde cross-linking experiments were also carried out. In the first experiment, a significant portion of the labeled 36-kDa IE110(3C) polypeptide containing codons 518 to 775 migrated on SDS-gels as a 75-kDa species after cross-linking (solid arrowhead, Fig. 5A, lanes 5 to 8). This result occurred both before and after immunoprecipitation and is consistent with a dimeric structure. Additional specific bands in the 160- to 240-kDa size range may also indicate formation of some tetrameric or larger multimeric forms (open arrowhead). Importantly, a 40-kDa truncated form of the HA-tagged IE110(3N) protein containing codons 245 to 518 failed to give immunoprecipitable dimers at similar protein concentrations in a parallel negative control cross-linking assay (Fig. 5A, lanes 1 to 4). Another HA-tagged IE110(3N) segment encoding a 43-kDa protein containing IE110 amino acids 245 to 552 was also negative in this type of assay (Fig. 5C and data not shown). These results revealed that the effect was specific for the C terminus of IE110 and that it was not an artifact created by the HA tag; however, they did not preclude the possibility of cross-linking to a cellular protein.

Therefore, in a second set of experiments, we examined whether two cotranslated polypeptides of different sizes could be cross-linked together to yield an intermediate-size heterodimer type of product. The results shown in Fig. 5B revealed that indeed such a heterodimer (HL) can be demonstrated. As before, HA_2/IE110(518–775) on its own gave an immunoprecipitable homodimer (HH) and larger forms after cross-linking (Fig. 5B, lanes 1 to 4). Similarly, a 29-kDa untagged form of IE110(3C) containing amino acids 555 to 775 produced a smaller cross-linked homodimer (LL) that could not be immunoprecipitated with the HA MAb (Fig. 5B, lanes 5 to 8). Finally, when the two were cotranslated, an additional cross-linked species of intermediate mobility (HL) appeared as well as the two parent homodimer forms (Fig. 5B, lanes 9 to 12). The new HL species (solid arrowhead) was immunoprecipitated with the HA MAb (lane 12), and we conclude that it represents a cross-linked heterodimer containing one subunit each of the HA_2/IE110(518–775) and the IE110(555–775) polypeptides. Interestingly, some of the cross-linked LL homodimers also appeared to immunoprecipitate in the presence of the HH and HL forms, which implies that they may have been part of a larger multimeric structure. Furthermore, in this experiment in particular, the proportion of the untagged 29-kDa subunit that was immunoprecipitated in the presence of the tagged 36-kDa subunit appeared to be even greater than the theoretical maximum of 50% for a simple dimer stoichiometry of 1:1:1:1 for HH, HL, LH, and LL subunits (Fig. 5B; compare lanes 9 and 10 or lanes 11 and 12).

Overall, these results provide unambiguous evidence that most of the IE110(3C) polypeptides synthesized in vitro are present in solution as stable dimers or higher-order structures and that there are direct cross-linkable contacts between the paired subunits.

Outer boundaries of the dimerization domain in IE110. To

map the C-terminal edge of the dimerization domain detected in vitro, we made a set of T7 polymerase-generated truncated RNAs from the untagged 68-kDa IE110(exon3) gene (Fig. 6C) and then translated them in reticulocyte lysates either alone or together with the 36-kDa HA-tagged IE110(3C) RNA. None of the six IE110(exon3) proteins tested, which terminated at codons 775 (*Eco*RI), 767 (*Sal*I), 711 (*Bst*EII), 552 (*Aat*II), 518 (*Mlu*I), and 392 (*Not*I), were precipitated on their own with the HA antibody in the absence of the cotranslated tagged protein (Fig. 6A, lanes 9 to 14). However, the two untagged proteins that terminated at codons 775 and 767 were both coprecipitated efficiently in the presence of the HA/IE110(3C) protein (solid arrowhead, Fig. 6B, lanes 9 and 10), whereas the truncations at 552, 518, and 392 failed to coprecipitate under these conditions (open arrowheads, Fig. 6B, lanes 12 to 14). The protein that terminated at codon 711 gave a positive result, but did so with only 25 to 30% of the efficiency of the larger forms (Fig. 6B, lane 11).

A second experiment carried out with truncations of the 36-kDa IE110(3C) protein starting at position 518 and ending at position 775 (*Eco*RI), 767 (*Sal*I), 714 (*Pml*I), 711 (*Bst*I), or 615 (*Sfi*I) gave similar results (Fig. 7C), although this time both the IE110(518–711) and IE110(518–714) proteins were coimmunoprecipitated with approximately 10% of the efficiency shown by the IE110(518–767) and IE110(518–775) forms (Fig. 7B, lanes 8 to 11). Again, none of these forms were precipitated in the absence of the tagged target protein (Fig. 7A, lanes 8 to 11). Therefore, the C-terminal boundary of the oligomerization domain lies inside codon 712, although the absence of codons 715 to 767 clearly has a large deleterious effect on the efficiency of the interaction.

The N-terminal boundary of the IE110 dimerization domain was also examined in this type of assay by using ^{35}S-labeled in vitro-translated proteins generated from new plasmid constructions that initiated at codon 555 (*Aat*II), 617 (*Sfi*I), 671 (*Xcm*I), or 680 (*Bsi*WI) and ended at codon 775 (Fig. 8C). In comparison with HA_2/IE110(518–775), none of these species reacted with the HA MAb on their own (Fig. 8A, lanes 7 to 10). However, both IE110(555–775) and IE110(617–775), but not IE110(671–775) or IE110(680–775), were coprecipitated after being cotranslated with HA_2/IE110(518–775) (solid arrowheads, Fig. 8B, lanes 7 to 10). Again, the smaller of these two positive dimerizing forms was immunoprecipitated with severalfold-lower efficiency than the larger one (compare Fig. 8, lanes 7 and 8).

Overall, these results revealed that a minimal dimerization domain that is functional in vitro maps between IE110 amino acids 617 and 711, with additional significant contributions to the efficiency of the interaction being provided by inclusion of amino acids 555 to 616 on the N-terminal side and 712 to 767 on the C-terminal side.

Detection of IE110 self-interactions by far-Western blotting. As an alternative approach to examining self-interactions between subunits of the C terminus of HSV-1 IE110, we also prepared a bacterial GST/IE110(3C) fusion protein (expected size, 62 kDa) containing the region encompassing codons 518 to 775. This construction yielded a soluble 57-kDa protein that could be partially purified by an affinity procedure using a glutathione-Sepharose column yielding three predominant polypeptide bands after Coomassie blue staining (Fig. 9A, lane 4). Parallel samples of this protein and a number of negative control proteins including other similar GST fusions (Fig. 9A, lanes 1, 2, 3, 5, 6, and 7) were fractionated on an SDS-polyacrylamide gel, transferred to a nitrocellulose membrane by electroblotting, and subjected to a denaturation and renaturation protocol (34). The far-Western blot was then incu-

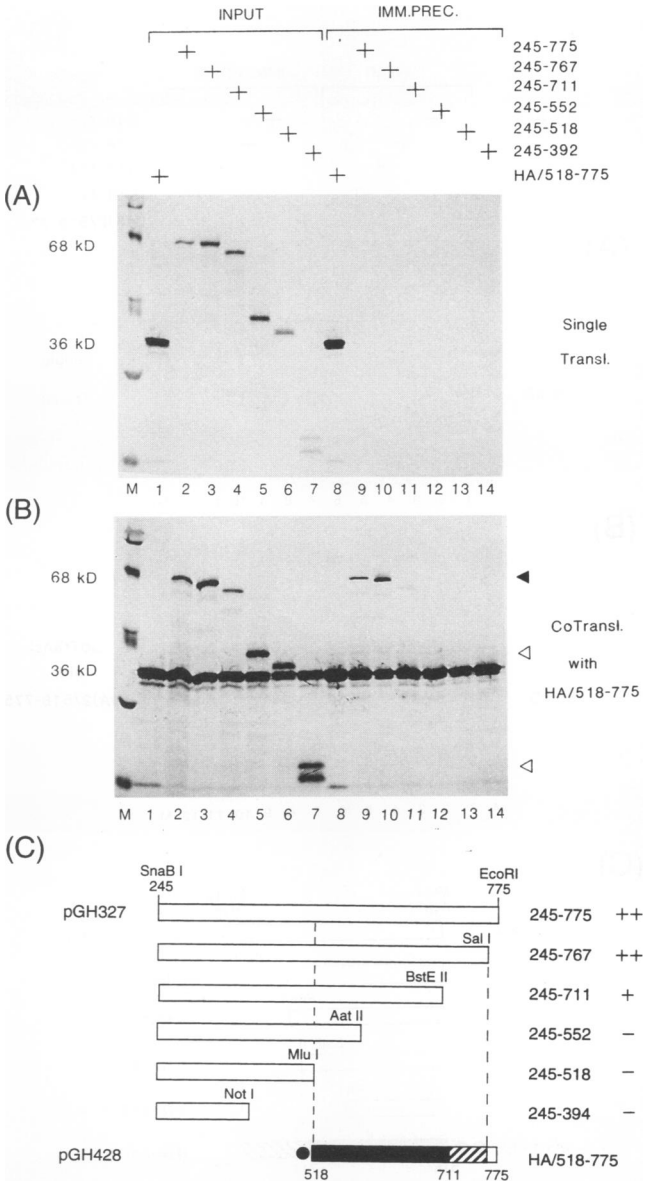

FIG. 6. Immunoprecipitation of cotranslated IE110(exon3) C-terminal truncated proteins. Plasmid pGH327 DNA encoding the untagged intact IE110(exon3) polypeptide was cleaved with various restriction enzymes before generation of truncated RNA with T7 polymerase followed by in vitro translation in rabbit reticulocyte lysate in the presence or absence of admixed RNA encoding the HA-tagged IE110(3C) polypeptide. (A) Single translation (Transl.) products. (B) Cotranslation (CoTransl.) with HA/IE110(518–775) from *Eco*RI-linearized pGH428. Lanes: 1 to 7, input [^{35}S]Met-labeled polypeptides analyzed before immunoprecipitation (IMM. PREC.); 8 to 14, parallel samples after immunoprecipitation with HA MAb; M, ^{14}C-labeled protein size markers; 1 and 8, tagged control 36-kDa HA/IE110(518–775) from pGH428(*Eco*RI); 2 and 9, untagged 68-kDa IE110(245–775) from pGH327(*Eco*RI); 3 and 10, IE110(245–767) from pGH327(*Sal*I); 4 and 11, IE110(245–711) from pGH327(*Bst*EII); 5 and 12, IE110(245–552) from pGH327(*Aat*II); 6 and 13, IE110(245–517) from pGH327(*Mlu*I); 7 and 14, IE110(245–392) from pGH327(*Not*I). Solid and open arrowheads denote the general positions of untagged forms of IE110(exon3) proteins in panel B that do and do not coprecipitate, respectively. (C) Diagram illustrating the structures of the polypeptides used in panels A and B. ++, +, and − indicate relative coimmunoprecipitation efficiency. Solid and hatched bars denote the interpretation of minimal and accessory regions for dimerization.

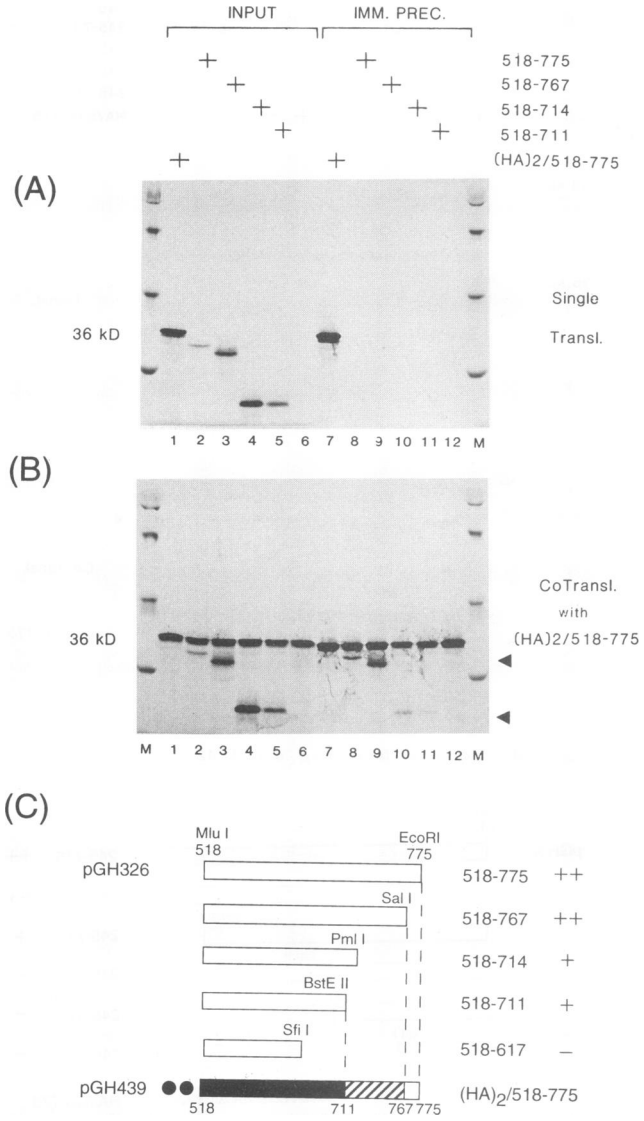

FIG. 7. Immunoprecipitation mapping of cotranslated IE110(3C) C-terminal truncated proteins. Plasmid pGH326 DNA encoding untagged IE110(518–775) was cleaved with various restriction enzymes before generation of RNA and in vitro translation in the presence or absence of admixed RNA encoding HA-tagged IE110(3C). (A) Single translation (Transl.) products. (B) Cotranslation (CoTransl.) with HA_2/IE110(518–775) from pGH439 (*Eco*RI linearized). Lanes: 1 to 6, input [^{35}S]Met-labeled polypeptides analyzed before immunoprecipitation (IMM. PREC.); 7 to 12, parallel samples after immunoprecipitation with HA MAb; M, ^{14}C-labeled size marker proteins; 1 and 7, tagged control 36-kDa HA_2/IE110(518–775) from pGH439(*Eco*RI); 2 and 8, untagged IE110(518–775) from pGH326(*Eco*RI); 3 and 9, IE110(518–767) from pGH326(*Sal*I); 4 and 10, IE110(518–714) from pGH326(*Pml*I); 5 and 11, IE110(518–711) from pGH326(*Bst*EII); 6 and 12, IE110(518–615) from pGH326(*Sfi*1) (which gave a 21-kDa product that was too small to be detectable on this gel). Arrowheads denote the positions of untagged forms of IE110(3C) proteins that coprecipitate. (C) Diagram illustrating the structures and relative coimmunoprecipitation efficiencies of polypeptides used in panels A and B. Solid and hatched bars denote the interpretation of minimal and accessory regions for dimerization.

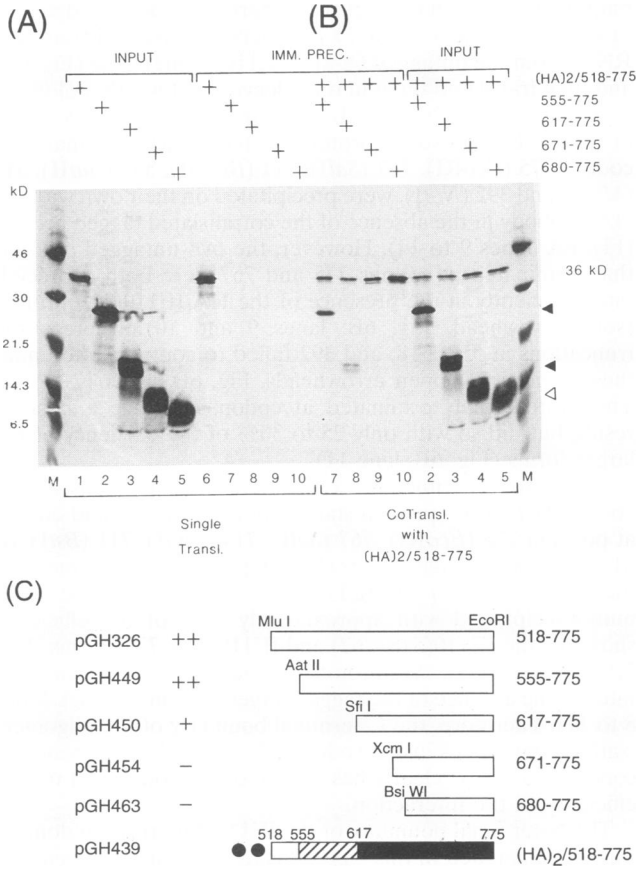

FIG. 8. Immunoprecipitation mapping of cotranslated IE110 (exon3) N-terminal truncated proteins. Four different untagged IE110 (3C)-derived in vitro-expression plasmids were cleaved with *Eco*RI for generation of RNA and synthesis of ^{35}S-labeled proteins in the presence or absence of admixed RNA encoding the 36-kD HA-tagged IE110(3C) protein. (A) Single translations (Transl.). (B) Cotranslation (CoTransl.) with HA_2/IE110(518–775) from *Eco*RI-linearized pGH439. Proteins were fractionated on an SDS–13.5% polyacrylamide gel. Lanes: 1 to 5, single or cotranslated input protein products before immunoprecipitation (IMM. PREC.); 6 to 10, single or cotranslated products after immunoprecipitation with HA MAb; M, ^{14}C-labeled size marker proteins; 1 and 6, tagged control 36-kDa HA_2/IE110(518–775) from pGH439(*Eco*RI); 2 and 7, untagged IE110(555–775) from pGH449(*Eco*RI); 3 and 8, IE110(617–775) from pGH450(*Eco*RI); 4 and 9, IE110(671–775) from pGH454(*Eco*RI); 5 and 10, IE110(680–775) from pGH463(*Eco*RI). Solid and open arrowheads indicate the positions of untagged forms of IE110(3C) that do and do not coprecipitate, respectively. (C) Diagram illustrating the structures and relative coimmunoprecipitation efficiencies of the polypeptides used in panels A and B above. Solid and hatched bars denote the interpretation of minimal and accessory domains for dimerization.

bated with a sample of the untagged ^{35}S-labeled in vitro-translated IE110(3C) polypeptide under conditions that we had determined eliminated any nonspecific interactions.

The results revealed a strong positive signal with the GST/IE110(3C) band only (Fig. 9B, lane 4) and no detectable reaction with any of the control protein bands, including GST itself, BSA, and several other GST fusion proteins such as GST/IE110(exon 2), GST/IE110(3N), GST/TBP(N), and GST/TBP(C) (Fig. 9B, lanes 1, 2, 3, 5, 6, and 7). The IE110(3C) probe detected both the major 57-kDa band and an additional

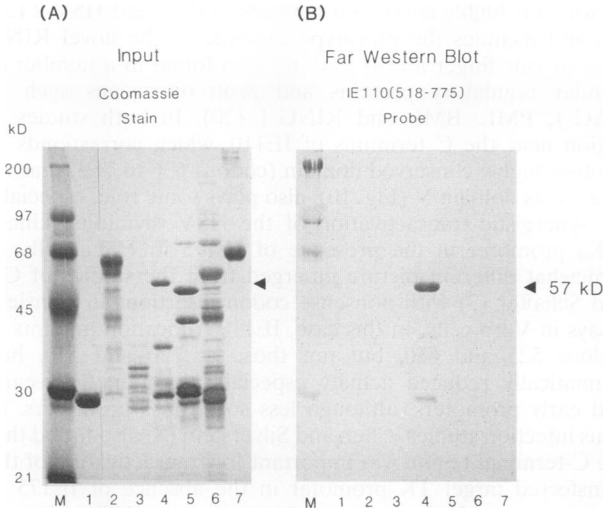

FIG. 9. Self-interaction of the IE110 C-terminal domain detected by a far-Western blotting procedure. A series of *E. coli*-produced GST fusion proteins and controls were fractionated by SDS–10% polyacrylamide gel electrophoresis, transferred to a nitrocellulose membrane by electroblotting, and subjected to a renaturation protocol. The membrane was then incubated with a sample of in vitro-translated ^{35}S-labeled IE110(exon3) polypeptide containing codons 518 to 775 that was synthesized in a rabbit reticulocyte extract from RNA generated from plasmid pGH326(*Eco*RI cleaved). (A) Coomassie blue-stained version of the gel. (B) Parallel autoradiograph of incubated and washed membrane version. Lanes: M, unlabeled and ^{14}C-labeled rainbow reference proteins; 1, GST; 2, GST/IE110(exon 2); 3, GST/IE110(3N); 4, GST/IE110(3C); 5, GST/TBP-N; 6, GST/TBP-C; 7, BSA. Protein sizes are marked on the left. The position of intact 57-kDa GST/IE110(3C) is indicated by the arrowhead.

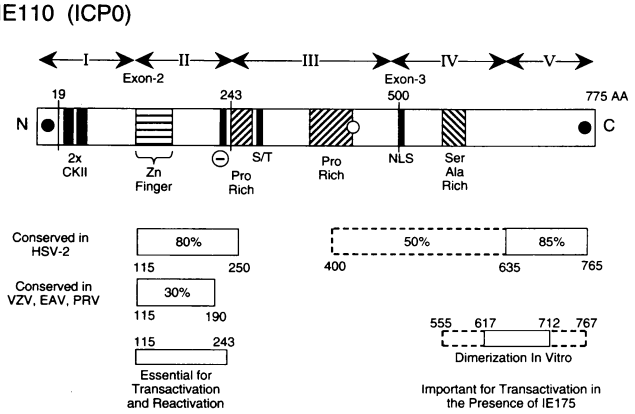

FIG. 10. Summary diagram illustrating known structural and functional features of the HSV-1 IE110 protein relative to conserved blocks (domains I to V) in the equivalent proteins of other alphaherpesviruses. Solid and shaded vertical bars denote potentially interesting structural motifs or regions. NLS, nuclear localization signal; S/T, serine- and threonine-rich block; CKII, potential consensus casein kinase motif. Map positions of the epitopes for the N- and C-terminal rabbit PAb and the H1083 MAb are indicated (solid and open circles, respectively). Boundary amino acid positions for mapped exons, structural domains, and functional properties are numbered. Primary nucleotide sequence data are derived from the following sources: HSV-1 IE110 (45); HSV-2 IE118 (35); varicella-zoster virus (VZV) gene 61 (13); pseudorabies virus (PRV) EP0 gene (10); and equine abortion virus (EHV-1) gene 63 (52).

minor 30-kDa band (Fig. 9B, lane 4). However, the latter was much less abundant in other preparations of GST/IE110(3C) and appears to represent a degradation product derived from the 57-kDa form. As a negative control, an unprogrammed reticulocyte lysate sample probe containing an equal amount of [^{35}S]Met-labeled protein failed to give any significant autoradiographic signal with a parallel membrane blot containing the same panel of GST and control proteins (not shown). The ability of IE110(3C) to interact with itself in this type of experiment may be feasible either because of some measurable level of dissociation and re-formation of the probe subunits at these high protein concentrations or because of some form of specific higher-order multimerization interactions between native (i.e., dimeric) forms of the IE110 C-terminal polypeptides.

DISCUSSION

Our evidence that IE110 forms stable homodimers in solution rests on the results of four independent types of experiments: intracellular colocalization, coimmunoprecipitation, cross-linking, and far-Western blotting. Initially, we used both single- and double-label IFA approaches to show that an IE175/IE110 hybrid protein (containing IE110 codons 313 to 775 tagged with an IE175 N-terminal epitope) was redistributed when cotransfected with the native intact 775-amino-acid IE110 protein. Furthermore, the hybrid protein exactly colocalized with an HA-tagged form of the nuclear punctate IE110 protein. The effect was dramatic and efficient, occurring in virtually every Vero and 293 cell that expressed both proteins. Furthermore, the wild-type IE110 punctate phenotype was clearly dominant in the hetero-oligomeric complexes over the irregular diffuse localization pattern observed with the nonpunctate hybrid protein subunits on their own. Note that in control experiments presented elsewhere (25, 38), we have found this type of effect to be specific in that the presence of IE110 punctate granules has no influence on the localization of several other cotransfected nonpunctate nuclear proteins that have been tested such as human cytomegalovirus IE1 or HSV ICP8. Most significantly, the IFA pattern of the IE175(N)-tagged IE110 hybrid protein varied according to which type of punctate pattern was displayed by the particular IE110 version that was used for cotransfection (i.e., nuclear, cytoplasmic, round, or elongated). Mapping studies revealed that a necessary domain within the wild-type IE110 protein for colocalization with the hybrid protein in DNA-transfected cells involved amino acids lying between codons 518 and 767.

The cotransfection results showed that self-interaction of the IE110 C-terminal segment occurs under intracellular conditions and not just in vitro or with the purified protein, but they did not address the question of whether the interaction is direct rather than possibly being mediated by a cellular protein. On the other hand, the coimmunoprecipitation of in vitro-translated products demonstrated the effect more directly and mapped the N- and C-terminal boundaries of the interaction domain to between IE110 codons 555 and 617 and codons 712 and 767 (Fig. 10). Furthermore, the ^{35}S-labeled untagged protein coprecipitated very efficiently with the HA epitope-tagged protein only after the two were cotranslated, not when they were simply mixed together. Therefore, a high-affinity subunit interaction mechanism with a low dissociation rate must be involved. Presumably, the two types of subunits are stably folded together during or directly after translation. Interestingly, both the colocalization and immunoprecipitation experiments gave only weak positive results with forms of IE110 that were truncated at position 711 (i.e., the interactions

occurred at only 10 to 20% of the efficiency displayed by wild-type forms), which tends to support the idea that the two types of assay are measuring essentially the same phenomenon.

The results of the cross-linking experiments with different-size in vitro-translated forms of the IE110 protein provided direct evidence for the presence of IE110 homodimers and heterodimers. Evidently, the individual subunits within paired dimers must be in direct physical contact even at low protein concentrations, and again only the C-terminal, not the N-terminal, domain displayed this property. Both the relatively low proportion of dimers and the formation of larger structures by cross-linking, together with the extraordinary dominance of the punctate over nonpunctate versions in the co-transfection assays, imply that higher oligomer formation is also very likely.

Finally, the far-Western blots revealed surprisingly efficient and specific protein-protein interactions between the labeled in vitro-translated IE110 C-terminal domain and an *E. coli*-expressed GST fusion protein containing the same region of IE110 after it had been denatured in SDS and renatured on a membrane matrix. We do not know at present whether the success of the far-Western blotting approach provides evidence for higher-order interactions between native forms of the protein or whether the higher protein concentrations achieved in this type of experiment permit subunit exchange. Alternatively, because of the denaturation and renaturation steps, it may be possible to drive the refolding of individual subunits of the IE110 domain into new heterodimers with the probe protein subunits during this type of experiment. Whatever the explanation, the use of *E. coli*-expressed IE110 protein in an SDS-gel almost certainly eliminates any possibility that additional cellular proteins are necessary to mediate the interactions.

Two previous studies have implied that the intact IE110 protein may be capable of forming multimerization interactions. Everett et al. (18) made this deduction from glycerol gradient centrifugation with partially purified protein from baculovirus-infected cells, and they also showed direct evidence from glutaraldehyde cross-linking for dimerization of a subset of their partially purified baculovirus protein. Chen et al. (7) have also argued for multimerization of wild-type IE110 from virus-infected cells on the basis of Sephacryl chromatography elution profiles and also because of the ability of several mutant forms of the protein to act as dominant negative competitors with the wild-type protein in functional assays involving transactivation and complementation. However, they predicted that the multimerization domain mapped at the N terminus of the protein and found that several C-terminal deletions still showed dominant competitive properties. Weber and Wigdahl (54) have also reported evidence for dominant negative IE110 mutants. Although such properties often do correlate with the ability to multimerize, this is not necessarily the case and more complicated explanations may be plausible. Furthermore, our results do not completely exclude the possibility of another dimerization or oligomerization domain within the N terminus or exon 2 of IE110 in addition to the C-terminal one that we have identified here.

Several previous studies have addressed aspects of the intracellular localization and transactivation functions of IE110 in detail, using various types of mutants in transient assays (3, 9, 15). The two studies using insertion and deletion mutants (9, 15) agree that the Cys-rich domain and a region to the right of it in exon 2 are of critical importance for transactivation of viral immediate-early, delayed-early, and late class promoters in both Vero and HeLa cells (Fig. 10). This region of the IE110 protein corresponds closely to domain II, which is highly conserved between HSV-1 and HSV-2 (35, 45) and includes the prototype example of the novel RING class of zinc finger motifs that are also found in a number of cellular regulatory proteins and proto-oncogenes such as RAG-1, PML, BMI, and RING-1 (20). In both studies, a region near the C terminus of IE110, which corresponds to another highly conserved domain (codons 636 to 769) that we refer to as domain V (Fig. 10), also plays some role, especially for synergistic transactivation of the HSV thymidine kinase (TK) promoter in the presence of IE175 in HeLa cells. A somewhat different picture emerged from the studies of Cai and Schaffer (3) with nonsense codon insertions in transient assays in Vero cells. In this case, IE110 truncation mutants at codons 525 and 680, but not those at 720 and 770, had dramatically reduced activity especially on immediate-early and early promoters, although less so on late promoters. In virus infection studies, Chen and Silverstein (8) also found that the C-terminal region was important for transactivation of the transfected target TK promoter in the absence of IE175 in both Vero and HeLa cells and for activation of TK-chloramphenicol acetyltransferase in the presence of IE175 in HeLa cells but not in Vero cells. In the latter studies, the functionally important C-terminal region in the HSV-1 IE110 protein lay between amino acids 628 and 697, which corresponds closely to our identified dimerization domain between codons 617 and 718.

Although only the N terminus of IE110 can transfer a punctate phenotype to hybrid IE110/IE175 proteins (38), the C terminus of IE110 is also necessary for efficient expression of the typical punctate localization phenotype in the intact IE110 protein (9, 16). From that observation, together with the genetic evidence for an ancillary role of the C-terminal region in transactivation properties and the highly conserved nature of the amino acids within domain V between HSV-1 and HSV-2 (35), we infer that dimerization plays an important role in the correct functioning of the HSV IE110 protein. As yet, we can discern no obvious known structural features, such as leucine zipper, helix-loop-helix, or zinc finger motifs, within the minimal 95-amino-acid dimerization block that would suggest a contribution to these properties. Further mapping is in progress so that the contribution from dimerization per se can be dissociated from other types of interactions and activities during future mapping studies of functional domains within the IE110 transactivator protein.

The region of IE110 that appears to interact with wild-type IE175 in colocalization studies (25, 38) overlaps with the dimerization domain described here. Both interactions are specific to the extent that they do not occur with several other cotransfected nuclear proteins tested, but the IE110 self-interaction also differs from the IE175-IE110 interaction by occurring in both Vero and 293 cells, whereas we could detect the latter only in Vero cells, not in 293 cells (37). It is also important to note that the domain of IE175 involved in IE110 interactions (25, 37) was not present in the IE175(1–383)/IE110(312–775) hybrid protein used here to demonstrate IE110 self-interactions by IFA. It seems probable that IE110 dimerization is needed for IE110-IE175 complexes to form, since the latter are not simple heterodimers, as judged by our inability to detect them by in vitro cotranslation procedures (37). However, we have no direct evidence to support this idea as yet and are currently attempting to generate mutations that will discriminate between these two types of IE110 protein-protein interactions.

It seems curious that although the C terminus of IE110 is relatively well conserved in HSV-1 and HSV-2, there is no residual homology outside the zinc finger domain between

either HSV protein and the equivalent proteins from other alpha herpesviruses such as varicella-zoster virus (13), pseudorabies virus (10), and equine abortion virus (or equine herpesvirus 1) (52). Perhaps this protein in HSV has developed additional functions involving dimerization and IE110-IE175 interactions that are not shared in the other viruses. One potential role of IE110 may be to bypass specific cell cycle requirements for progression into the lytic cycle (4) and another might be to assist the IE175 transactivator in accessing nucleosome-covered viral delayed-early promoters during reactivation from the latent state in the absence of VP16 (2, 3).

ACKNOWLEDGMENTS

These studies were funded by DHEW research grants RO1 CA28473 and R37 CA22130 to G.S.H. from the National Cancer Institute. M.-A.M. was a visiting graduate student from the Department of Chemistry at the University of South Carolina.

We thank Beverly Lambe, Mabel Chiu, and Susan Gerstberger for technical assistance at various times with some of the recombinant DNA constructions, plasmid DNA preparations, and IFA, and we thank Sarah Heaggans and Pamela Wright for secretarial and photographic assistance in preparation of the manuscript.

REFERENCES

1. **apRhys, C., D. M. Ciufo, E. A. O'Neill, T. J. Kelly, and G. S. Hayward.** 1989. Overlapping octamer and TAATGARAT motifs in the VF65-response elements in herpes simplex virus immediate-early promoters represent independent binding sites for cellular nuclear factor III. J. Virol. **63:**2798–2812.
2. **Bachenheimer, S. L., and N. Elshiekh.** 1990. Variable requirements for herpes simplex virus immediate-early proteins in the expression of the adenovirus E2 gene. Virology **175:**338–342.
3. **Cai, W., and P. A. Schaffer.** 1989. Herpes simplex virus type 1 ICP0 plays a critical role in the de novo synthesis of infectious virus following transfection of viral DNA. J. Virol. **63:**4579–4589.
4. **Cai, W., and P. A. Schaffer.** 1991. A cellular function can enhance gene expression and plating efficiency of a mutant defective in the gene for ICP0, a transactivating protein of herpes simplex virus type 1. J. Virol. **65:**4078–4090.
5. **Cai, W., and P. A. Schaffer.** 1992. Herpes simplex virus type 1 ICP0 regulates expression of immediate-early, early, and late genes in productively infected cells. J. Virol. **66:**2904–2915.
6. **Chang, Y.-N., D. L.-Y. Dong, G. S. Hayward, and S. D. Hayward.** 1990. The Epstein-Barr virus Zta transactivator: a member of the bZIP family with unique DNA-binding specificity and a dimerization domain that lacks the characteristic heptad leucine zipper motif. J. Virol. **64:**3358–3369.
7. **Chen, J., C. Panagiotidis, and S. Silverstein.** 1992. Multimerization of ICP0, a herpes simplex virus immediate-early protein. J. Virol. **66:**5598–5602.
8. **Chen, J., and S. Silverstein.** 1992. Herpes simplex viruses with mutations in the gene encoding ICP0 are defective in gene expression. J. Virol. **66:**2916–2927.
9. **Chen, J., X. Zhu, and S. Silverstein.** 1991. Mutational analysis of the sequence encoding ICP0 from herpes simplex virus type 1. Virology **180:**207–220.
10. **Cheung, A. K.** 1991. Cloning of the latency gene and the early protein 0 gene of pseudorabies virus. J. Virol. **65:**5260–5271.
11. **Ciufo, D. M., C. apRhys, M. S. Roberts, and G. S. Hayward.** 1988. Viral and cellular factors involved in the regulation of the IE175 and IE110 promoters of herpes simplex virus, p. 95–111. Proceedings of the Symposium on Regulation of Viral Gene Expression. George Khoury Educational Foundation, Inc.
12. **Dasmahapatra, B.** 1993. A novel cell free expression vector: use of an insect virus translational initiation signal for *in vitro* gene expression. Methods Enzymol. **217:**143–151.
13. **Davison, A. J., and J. E. Scott.** 1986. The complete DNA sequence of varicella-zoster virus. J. Gen. Virol. **67:**1759–1816.
14. **Everett, R. D.** 1984. Transactivation of transcription by herpes virus products: requirement for two HSV-1 immediate-early polypeptides for maximum activity. EMBO J. **3:**3135–3141.
15. **Everett, R. D.** 1987. A detailed mutational analysis of Vmw110, a trans-acting transcriptional activator encoded by herpes simplex virus type 1. EMBO J. **6:**2069–2076.
16. **Everett, R. D.** 1988. Analysis of the functional domains of herpes simplex virus type 1 immediate-early polypeptide Vmw110. J. Mol. Biol. **202:**87–96.
17. **Everett, R. D.** 1988. Promoter sequence and cell type can dramatically affect the efficiency of transcriptional activation induced by herpes simplex virus type 1 and its immediate-early gene products Vmw175 and Vmw110. J. Mol. Biol. **203:**739–751.
18. **Everett, R. D., A. Orr, and M. Elliott.** 1991. High level expression and purification of herpes simplex virus type 1 immediate early polypeptide Vmw110. Nucleic Acids Res. **19:**6155–6161.
19. **Field, J., J.-I. Nikawa, D. Broek, B. MacDonald, L. Rodgers, I. A. Wilson, R. A. Lerner, and M. Wigler.** 1988. Purification of a *ras*-responsive adenyl cyclase complex from *Saccharomyces cerevisiae* by the use of an epitope addition method. Mol. Cell. Biol. **8:**2159–2165.
20. **Freemont, P. S., I. M. Hanson, and J. Trowsdale.** 1991. A novel cysteine rich sequence motif. Cell **64:**483–484.
21. **Gelman, I. H., and S. Silverstein.** 1985. Identification of immediate early genes from herpes simplex virus that transactivates the virus thymidine kinase gene. Proc. Natl. Acad. Sci. USA **82:**5265–5269.
22. **Gelman, I. H., and S. Silverstein.** 1986. Co-ordinate regulation of herpes simplex virus gene expression is mediated by the functional interaction of two immediate early gene products. J. Mol. Biol. **191:**395–409.
23. **Gelman, I. H., and S. Silverstein.** 1987. Herpes simplex virus immediate-early promoters are responsive to virus and cell *trans*-acting factors. J. Virol. **61:**2286–2296.
24. **Hagemeier, C., S. Walker, R. Caswell, T. Kouzarides, and J. Sinclair.** 1992. The human cytomegalovirus 80-kilodalton but not the 72-kilodalton immediate-early protein transactivates heterologous promoters in a TATA-box-dependent mechanism and interacts directly with TFIID. J. Virol. **66:**4452–4456.
25. **Harrigan-Mullen, M.-A.** 1991. Characterization of nuclear translocation, dimerization and IE110-IE175 interaction domains of the IE110 and IE175 proteins of HSV-1. Ph.D. thesis. The University of South Carolina, Columbia.
26. **Harris, R. A., R. D. Everett, X. Zhu, S. Silverstein, and C. M. Preston.** 1989. Herpes simplex virus type 1 immediate-early protein Vmw110 reactivates latent herpes simplex virus type 2 in an in vitro latency system. J. Virol. **63:**3513–3515.
27. **Hay, R. T., and J. Hay.** 1980. Properties of herpesvirus-induced "immediate-early" polypeptides. Virology **104:**230–234.
28. **Hayward, G. S.** 1993. Immediate-early gene regulation in herpes simplex virus. Semin. Virol. **4:**15–23.

28a. **Hayward, G. S.** Unpublished data.

29. **Knipe, D. M., D. Senechek, S. A. Rice, and J. L. Smith.** 1987. Stages in the nuclear association of the herpes simplex virus transcriptional activator protein ICP4. J. Virol. **61:**276–284.
30. **Kolodziej, P. A., and R. A. Young.** 1991. Epitope tagging and protein surveillance. Methods Enzymol. **194:**508–519.
31. **LaFemina, R. L., M. C. Pizzorno, J. D. Mosca, and G. S. Hayward.** 1989. Expression of the acidic nuclear immediate-early protein (IE1) of human cytomegalovirus in stable cell lines and its preferential association with metaphase chromosomes. Virology **172:**584–600.
32. **Leib, D. A., D. M. Coen, C. L. Bogard, K. A. Hicks, D. R. Yager, D. M. Knipe, K. L. Tyler, and P. A. Schaffer.** 1989. Immediate-early regulatory gene mutants define different stages in the establishment and reactivation of herpes simplex virus latency. J. Virol. **63:**759–768.
33. **Lieberman, P. M., J. M. Hardwick, J. Sample, G. S. Hayward, and S. D. Hayward.** 1990. The Zta-transactivator involved in induction of lytic cycle gene expression in Epstein-Barr virus-infected lymphocytes binds to both AP-1 and ZRE sites in target promoter and enhancer regions. J. Virol. **64:**1143–1155.
34. **Lieberman, P. M., and A. J. Berk.** 1991. The Zta trans-activator protein stabilizes TFIID association with promoter DNA by direct protein-protein interaction. Genes Dev. **5:**2441–2454.
35. **McGeoch, D. J., C. Cunningham, G. McIntyre, and A. Dolan.** 1991.

Comparative sequence analysis of the long repeat regions and adjoining parts of the long unique regions in the genomes of herpes simplex virus types 1 and 2. J. Gen. Virol. **72**:3057–3075.

36. **Middleton, M. H., G. R. Reyes, D. M. Ciufo, A. Buchan, J. C. M. Macnab, and G. S. Hayward.** 1982. Expression of cloned herpesvirus genes. I. Detection of nuclear antigens from herpes simplex virus type 2 inverted repeat regions in transfected mouse cells. J. Virol. **43**:1091–1101.
37. **Mullen, M.-A., D. M. Ciufo, S. Gerstberger, and G. S. Hayward.** Unpublished data.
38. **Mullen, M.-A., D. M. Ciufo, and G. S. Hayward.** 1994. Mapping of intracellular localization domains and evidence for colocalization interactions between the IE110 and IE175 nuclear transactivator proteins of herpes simplex virus. J. Virol. **68**:3250–3266.
39. **Nagpal, S., and J. M. Ostrove.** 1991. Characterization of a potent varicella-zoster virus-encoded *trans*-repressor. J. Virol. **65**:5289–5296.
40. **Nakabeppu, Y., K. Ryder, and D. Nathans.** 1988. DNA-binding activities of three murine Jun proteins: stimulation by Fos. Cell **55**:907–915.
41. **O'Hare, P., and G. S. Hayward.** 1985. Evidence for a direct role for both the 175,000- and 110-000-molecular-weight immediate-early proteins of herpes simplex virus in the transactivation of delayed early promoters. J. Virol. **53**:751–760.
42. **O'Hare, P., and G. S. Hayward.** 1985. Three *trans*-acting regulatory proteins of herpes simplex virus modulate immediate-early gene expression in a pathway involving positive and negative feedback regulation. J. Virol. **56**:723–733.
43. **O'Hare, P., and G. S. Hayward.** 1987. Comparison of upstream sequence requirements for positive and negative regulation of a herpes simplex virus immediate-early gene by three virus-encoded *trans*-acting factors. J. Virol. **61**:190–199.
44. **O'Hare, P., J. D. Mosca, and G. S. Hayward.** 1986. Multiple trans-activating proteins of herpes simplex virus that have different target promoter specificities and exhibit both positive and negative regulatory functions. Cancer Cells **4**:175–188.
45. **Perry, L. J., F. J. Rixon, R. D. Everett, M. C. Frame, and D. J. McGeoch.** 1986. Characterization of the IE110 gene of herpes simplex virus type 1. J. Gen. Virol. **67**:2365–2380.
46. **Pizzorno, M. C., M.-A. Mullen, Y.-N. Chang, and G. S. Hayward.** 1991. The functionally active IE2 immediate-early regulatory protein of HCMV is an 80-kilodalton polypeptide that contains two distinct activator domains and a duplicated nuclear localization signal. J. Virol. **65**:3839–3852.
47. **Quinlan, M. P., and D. M. Knipe.** 1985. Stimulation of expression of a herpes simplex virus DNA-binding protein by two viral functions. Mol. Cell. Biol. **5**:957–963.
48. **Roberts, M. S., A. Boundy, P. O'Hare, M. C. Pizzorno, D. M. Ciufo, and G. S. Hayward.** 1988. Direct correlation between a negative autoregulatory response element at the cap site of the herpes simplex virus type 1 IE175 (α4) promoter and a specific binding site for the IE175 (ICP4) protein. J. Virol. **62**:4307–4320.
49. **Russell, J., N. D. Stow, E. C. Stow, and C. M. Preston.** 1987. Herpes simplex virus genes involved in latency in vitro. J. Gen. Virol. **68**:3009–3018.
50. **Sacks, W. R., and P. A. Schaffer.** 1987. Deletion mutants in the gene encoding the herpes simplex virus type 1 immediate-early protein ICP0 exhibit impaired growth in cell culture. J. Virol. **61**:829–839.
51. **Stow, N. D., and E. C. Stow.** 1986. Isolation and characterization of a herpes simplex virus type 1 mutant containing a deletion within the gene encoding the immediate-early polypeptide Vmw110. J. Gen. Virol. **67**:2571–2585.
52. **Telford, E. A., M. S. Watson, K. McBride, and A. J. Davison.** 1992. The DNA sequence of equine herpesvirus-1. Virology **189**:304–316.
53. **Towbin, H., T. Staehelin, and J. Gordon.** 1979. Electrophoretic transfer of proteins from polyacrylamide gels to nitrocellulose sheets: procedure and some applications. Proc. Natl. Acad. Sci. USA **76**:4350–4354.
54. **Weber, P. C., and B. Wigdahl.** 1992. Identification of dominant-negative mutants of the herpes simplex virus type 1 immediate-early protein ICP0. J. Virol. **66**:2261–2267.
55. **Zhu, X., J. Chen, and S. Silverstein.** 1991. Isolation and characterization of a functional cDNA encoding ICP0 from herpes simplex virus type 1. J. Virol. **65**:957–960.
56. **Zhu, X., J. Chen, C. S. H. Young, and S. Silverstein.** 1990. Reactivation of latent herpes simplex virus by adenovirus recombinants encoding mutant IE-0 gene products. J. Virol. **64**:4489–4498.
57. **Zhu, X., A. G. Papavassiliou, H. G. Stunnenburg, and S. Silverstein.** 1991. Transactivation by herpes simplex virus proteins ICP4 and ICP0 in vaccinia virus infected cells. Virology **184**:67–78.
58. **Zhu, X., C. S. H. Young, and S. Silverstein.** 1988. Adenovirus vector expressing functional herpes simplex virus ICP0. J. Virol. **62**:4544–4553.